Cardiac Positron Emission Tomography Imaging

Josef Machac, MD

Cardiac positron emission tomography (PET) imaging has advanced from primarily a research tool to a practical, high-performance clinical imaging modality. The widespread availability of state-of-the-art PET gamma cameras, the commercial availability of perfusion and viability PET imaging tracers, reimbursement for PET perfusion and viability procedures by government and private health insurance plans, and the availability of computer software for image display of perfusion, wall motion, and viability images have all been a key to cardiac PET imaging becoming a routine clinical tool. Although myocardial perfusion PET imaging is an option for all patients requiring stress perfusion imaging, there are identifiable patient groups difficult to image with conventional single-photon emission computed tomography imaging that are particularly likely to benefit from PET imaging, such as obese patients, women, patients with previous nondiagnostic tests, and patients with poor left ventricular function attributable to coronary artery disease considered for revascularization. Myocardial PET perfusion imaging with rubidium-82 is noteworthy for high efficiency, rapid throughput, and in a high-volume setting, low operational costs. PET metabolic viability imaging continues to be a noninvasive standard for diagnosis of viability imaging. Cardiac PET imaging has been shown to be cost-effective. The potential of routine quantification of resting and stress blood flow and coronary flow reserve in response to pharmacologic and cold-pressor stress offers tantalizing possibilities of enhancing the power of PET myocardial perfusion imaging. This can be achieved by providing assurance of stress quality control, in enhancing diagnosis and risk stratification in patients with coronary artery disease, and expanding diagnostic imaging into the realm of detection of early coronary artery disease and endothelial dysfunction subject to risk factor modification. Combined PET and x-ray computed tomography imaging (PET-CT) results in enhanced patient throughput and efficiency. The combination of multislice computed tomography scanners with PET opens possibilities of adding coronary calcium scoring and noninvasive coronary angiography to myocardial perfusion imaging and quantification. Evaluation of the clinical role of these creative new possibilities warrants investigation.
Semin Nucl Med 35:17-36 © 2005 Elsevier Inc. All rights reserved.

Why Cardiac Positron Emission Tomography (PET)?

Coronary artery disease (CAD) continues to be a leading cause of death in modern industrialized countries. A steady growth in the use of myocardial single-photon emission computed tomography (SPECT) perfusion imaging has been charted in the past 2 decades and, as a result, SPECT has become an important component of the clinical management of this disease. This is attributable to its high success rate in providing useful information about myocardial perfusion and function.

Despite the success of cardiac SPECT imaging, room for significant improvement still exists. Despite a high sensitivity of 90% to 94% for multivessel coronary disease, conventional SPECT imaging has a limited sensitivity of 60% to 76% for detecting significant single-vessel disease.[1,2] The presence of diffuse disease in all 3 coronary vessels may decrease the sensitivity for each individual vessel, and "balanced ischemia" may mask the presence of disease altogether.[3-7] Diffuse coronary artery disease without segmental stenosis frequently is the substrate for plaque rupture and coronary events.[8-10] Identification of early disease is a target of intervention through diet, glycemic control, lifestyle changes, and pharmacologic therapy.[11-16] The detection of preclinical coronary disease by conventional radionuclide imaging is limited by incomplete extraction of tracer by the myocardium

Department of Radiology, Mount Sinai School of Medicine, Mount Sinai Medical Center, New York, NY.
Address reprint requests to Josef Machac, MD, Mount Sinai Medical Center, Box 1141, Nuclear Medicine, 1 Gustave Levy Place, New York, NY 10029. E-mail: josef.machac@msnyuhealth.org

Table 1 Cardiac PET Tracers

Agent	Physical half-life[215]	Mean positron range (mm)[216-218]	Production	Extraction
^{13}N NH$_3$	10.0 min	0.7	Cyclotron	80%[219]
^{82}Rb	78 s	2.6	Generator	50-60%[220]
^{15}O H$_2$O	2.0 min	1.1	Cyclotron	Diffusible
^{18}F FDG	110 min	0.2	Cyclotron	1-3%[221]

during first passage[17-19] and by the absence of hemodynamically significant coronary obstruction.

The use of vasodilator stress agents like dipyridamole or adenosine, which are used in approximately 40% of all stress imaging procedures, does not provide independent information about the adequacy of the vasodilator stress. Despite a high overall effectiveness, the surreptitious use of caffeine, diffuse epicardial disease, or diffuse small vessel disease may contribute to slightly decreased negative prognostic predictive value of pharmacologic myocardial perfusion imaging compared with exercise.[20] Our reliance on relative regional deficiencies in perfusion may mask a uniformly poor response to vasodilatory stimulation.

SPECT imaging also is limited by artifacts stemming from nonuniform attenuation. The recognition of attenuation artifacts through intensive training, experience, and the use of gated SPECT imaging,[21] still leaves a frequent uncertainty about possible underlying CAD in the presence of artifact.[22,23]

Another area of possible improvement is the relative low efficiency of conventional gamma cameras. Coupled with a limit on the maximal dose of radiotracer, there is a lower limit on the time required for image acquisition. From the patient's point of view, common acquisition protocols take several hours to complete. The half-lives of currently used radioisotopes limit the number of repeat tracer injections.

Recent Changes in the Status of PET Imaging

Despite the fact that the clinical value of cardiac PET imaging was demonstrated 20 years ago,[24-26] its clinical use has been minimal. The clinical impracticality of PET included limitation to a few research centers, the need for a cyclotron, the expense of PET, lack of reimbursement, and limited availability of user-friendly software for cardiac image processing and display, with a few exceptions.

All of that has changed. With more than 1000 PET cameras installed in North America (GE Medical Systems, personal communication, 2004), there is an extensive infrastructure in PET imaging. With an average use of only 4 oncologic studies being performed per PET scanner per day (GE Medical Systems, personal communication, 2004), there is potential for part-time availability of most PET scanners for cardiac imaging. Myocardial PET perfusion imaging with rubidium-82 (^{82}Rb), reimbursed by the Center for Medicaid and Medicare Services (CMS) since 1995, is possible with a commercially available generator. Mobile ^{82}Rb generators are available in some regions for centers that choose to offer PET myocardial perfusion imaging only one to several times a week. ^{18}F fluorodeoxyglucose (FDG) PET imaging is now reimbursed for myocardial viability. Metropolitan areas in North America now have at least one commercial supplier of FDG. More recently, CMS reimbursement became available for myocardial perfusion imaging with ^{13}N ammonia.

The Power of PET Imaging

PET imaging differs from conventional radionuclide imaging because it uses radionuclides that decay with positron emission. A positron has the same mass as an electron but has a positive charge. The positron travels a short distance, up to a few millimeters, interacts with an electron, and the two undergo a mutual annihilation, resulting in the production of 2 511-kev gamma photons, 180° apart form each other. PET imaging consists of detection of these photons in coincidence. Imaging by PET with electronic coincidence localization using a ring detector leads to high acquisition efficiency. This results in high-quality images acquired in a short time and multiple sequential acquisitions. The short half-lives of ^{82}Rb and ^{13}N ammonia (Table 1) result in low radiation exposure for the patient (Table 2) from multiple intervention studies or follow-up studies and allow other radionuclide imaging studies on the same day. High image uniformity is a result of the ability of PET to perform effective nonuniform attenuation correction, thus minimizing attenuation artifact. The ability to calibrate the PET system allows quantification of myocardial flow and glucose utilization.

Table 2 Cardiac PET Tracer Dosimetry[222]

Agent	Activity (mCi)	EDE (rem)	Critical Organ	Organ Dose (rem)
^{13}N NH$_3$	20	0.166	Bladder	0.52
^{82}Rb	60	0.096[240]	Kidneys	1.98
^{15}O H$_2$O	60	0.252	Heart	0.49
^{18}F FDG	10	1.100	Bladder	7.00

Table 3 Imaging Protocol for ^{13}N Ammonia PET Imaging

Procedure	Time
Positioning (Scout)	5 min
Transmission imaging	10 min
Injection and blood clearance	5 min
Rest gated perfusion imaging	10-20 min
^{13}N decay waiting time	45 min
Pharmacological stress	7 min
Injection and blood clearance	5 min
Stress imaging	10-20 min
Total duration	100-120 min

PET imaging offers a potentially high resolution of 5 to 7 mm, compared with 15 mm with SPECT imaging,[27] although in cardiac imaging, resolution is degraded by respiratory and cardiac wall movement. Cardiac imaging offers some but not the full potential resolution of PET.

Myocardial PET Perfusion Tracers and Imaging Protocols

^{13}N Ammonia

The principal cardiac PET radiotracers are listed in Tables 1 and 2. ^{13}N ammonia has been used for most of the scientific investigations in cardiac PET imaging for the past 2 decades. Its 10-minute half-life requires an on-site cyclotron and radiochemistry synthesis capability. A sample imaging protocol is given in Table 3. Pharmacologic stress imaging usually follows resting injection and imaging, after the initial activity has been allowed to decay, by staggering patients, or using differential doses for rest and stress. Both rest and stress images can be gated. A dynamic acquisition is acquired for the quantification of blood flow. This can be accomplished by performing separate dynamic and gated acquisitions with the same injection, or through list-mode acquisition. A third injection may be included for cold-pressor testing. ^{13}N ammonia imaging requires coordinating the activities of at least 4 people; the cyclotron operator, the radiochemist, the PET technologist, and the supervising physician. It can be a daunting task with a large number of rest and stress ^{13}N ammonia studies on the same day.

In the bloodstream, ^{13}N ammonia consists of neutral ammonia (NH_3) in equilibrium with its charged ammonium (NH_4) ion. The neutral NH_3 molecule readily diffuses across plasma and cell membranes. Inside the cell, it re-equilibrates with its ammonium form, which is trapped in glutamine via the enzyme glutamine synthase.[28,29] Despite back diffusion, the first-pass trapping of ^{13}N ammonia at rest is high, although decreasing with higher blood flow.

^{13}N ammonia allows good quality gated and ungated images (Fig. 1), taking full advantage of the superior resolution of PET imaging. Interestingly, normal volunteers show mild heterogeneity or mild defects of ^{13}N ammonia retention in the lateral wall of the left ventricle compared with the other segments. The mechanism of this finding is not known.[30] This must be taken into account for both visual and quantitative analysis. ^{13}N ammonia images may be degraded by occasional intense liver activity, and increased lung activity in patients with lung congestion.[31]

Oxygen-15 (^{15}O) Water

^{15}O water is neither an approved tracer nor reimbursed for clinical imaging in the United States but is included in this review as an important tracer for quantitative investigations of myocardial blood flow.[32] The ability of water to diffuse freely across plasma membranes makes this tracer a favorite for quantitation of myocardial blood flow. However, this very property leads to poor contrast between the myocardium and cardiac blood pool, requiring subtraction of blood pool activity. The use of ^{15}O water is restricted to sites with a cyclotron.

Rubidium-82 (^{82}Rb)

^{82}Rb is produced in a commercially available generator by decay from strontium-82 attached to an elution column. ^{82}Rb is eluted with 25 to 50 mL of normal saline by a computer-controlled elution pump, connected by IV tubing to the patient. The strontium-82 containing generator is replaced every 4 weeks ($t_{1/2}$ = 25 days). ^{82}Rb decays by positron emission with a short half-life of 75 s (Table 1). The generator is fully replenished every 10 minutes, and 90% of maximal available activity can be obtained within 5 minutes after the last elution.[33] Whereas the short half-life of ^{82}Rb taxes the performance limits of PET scanners, it facilitates the rapid completion of a series of resting and stress myocardial perfusion studies (Tables 4 and 5). Thus, ^{82}Rb is a very efficient imaging agent for routine clinical usage. The fixed cost of the ^{82}Rb generator may be an initial hurdle. Although the cost per patient at a low volume of studies per day is high, the cost with 6 to 10 studies per day is competitive with SPECT tracers.

^{82}Rb, like thallium-201, is a cation and an analog of potassium. It is extracted from plasma by myocardial cells via the Na^+/K^+ ATPase pump. Myocardial extraction of ^{82}Rb is similar to thallium-201 (^{201}Tl)[34,35] and slightly less than N-13 ammonia (Table 1), decreasing during hyperemia.[36,37] ^{82}Rb extraction can be altered by severe acidosis, hypoxia, and
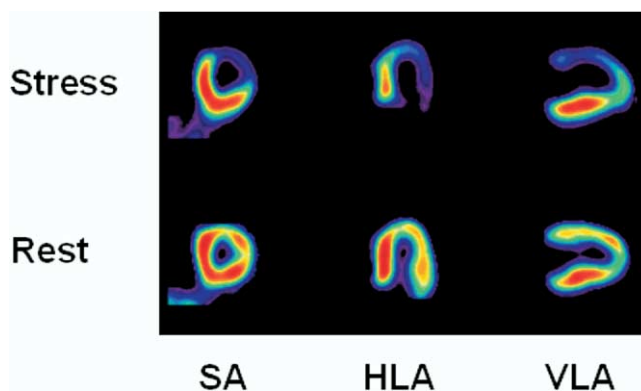
Figure 1 ^{13}N Ammonia PET images demonstrating anterior and lateral defects during pharmacological stress and significant improvement at rest, consistent with ischemia. SA, short axis; HLA, horizontal long axis; VLA, vertical long axis (courtesy of Dr. H Schelbert, UCLA School of Medicine, CA).

Table 4 Imaging Protocol for [82]Rb PET Imaging With a Bismuth Germanate (BGO) Crystal PET Scanner (the Mount Sinai Medical Center, NY)

Procedure	Time
Positioning (Scout)	5 min
Rest gated imaging	8 min
Rest perfusion imaging	8 min
Transmission imaging	8 min
Pharmacological stress	7 min
Stress imaging	8 min
Total duration	44 min

ischemia.[38-40] Thus, uptake of [82]Rb is a function of both blood flow and of myocardial cell integrity.

Patient Preparation and Stress Testing

Patient preparation for stress and rest myocardial PET perfusion imaging is identical to SPECT perfusion imaging. Myocardial PET perfusion imaging usually is performed with pharmacologic stress, primarily with dipyridamole or adenosine, despite the fact that ^{13}N ammonia imaging is feasible with treadmill stress testing and despite isolated satisfactory results with exercise using [15]O water[41] or [82]Rb.[42]

Imaging of [82]Rb

Despite the short half-life of [82]Rb, modern PET gamma cameras are able to obtain good quality images (Figs. 2 and 3). Imaging with [82]Rb does not take full advantage of the superior resolution of PET because of the relatively long mean path (2.6 mm) of the energetic [82]Rb positrons (Table 1) and due to the need for filtering with the short-lived tracer.

Our protocol (Table 4) begins with a low dose ([20m]Ci) injection of [82]Rb and a short 3-min scout acquisition and quick reconstruction for proper positioning. The patient then receives a 50- to 60-mCi dose at rest, acquired in 2D gated mode for 6 min beginning at 2 min after the onset of injection. This is followed by another 50- to 60-mCi injection, at rest, using a phasic (dynamic), 8-min acquisition, for perfusion imaging. The dynamic acquisition allows a retrospective selection of the onset of the myocardial phase, which is delayed in heart failure, low cardiac output, or poor bolus quality, and allows blood flow quantification. This is followed by an 8-min transmission scan with a germanium-68 pin source. The patient then undergoes pharmacologic stress. At peak

Table 5 Imaging Protocol for [82]Rb PET Imaging With Lutetium Orthosilicate (LSO) Crystal PET Scanner[223]

Procedure	Time
Rest transmission imaging	4 min
Rest perfusion 2D imaging	5 min
Rest gated 3D imaging	3 min
Pharmacological stress	7 min
Stress transmission imaging	4 min
Stress perfusion 2D imaging	5 min
Stress gated 3D imaging	3 min
Total duration	31 min
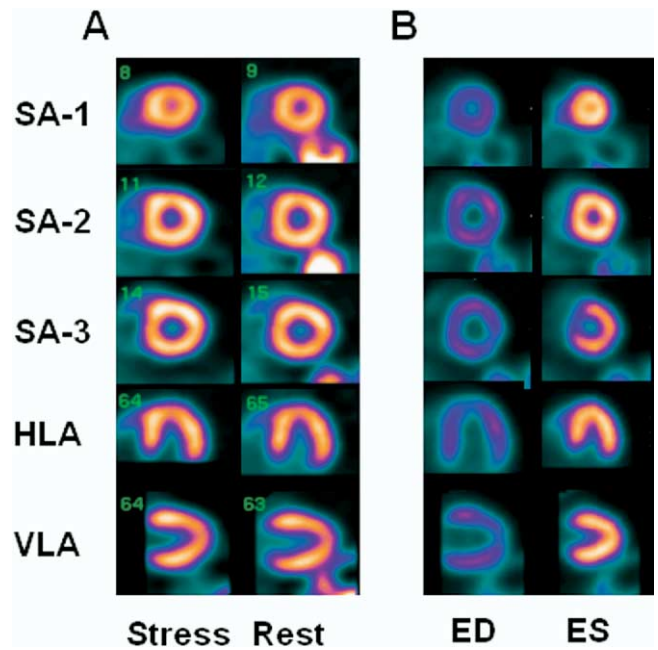
Figure 2 A, Normal stress and rest [82]Rb PET images. B, Resting end-diastolic (ED) and end-systolic (ES) gated images, showing uniformly good contractility.

stress, the patient is injected with the final 50- to 60-mCi [82]Rb dose, for an 8-min dynamic (phasic) acquisition. The total camera acquisition time is approximately 45 min. The need for repositioning, repeating an acquisition, or clinical factors may extend the required time.

For the rest and stress perfusion image reconstruction, we
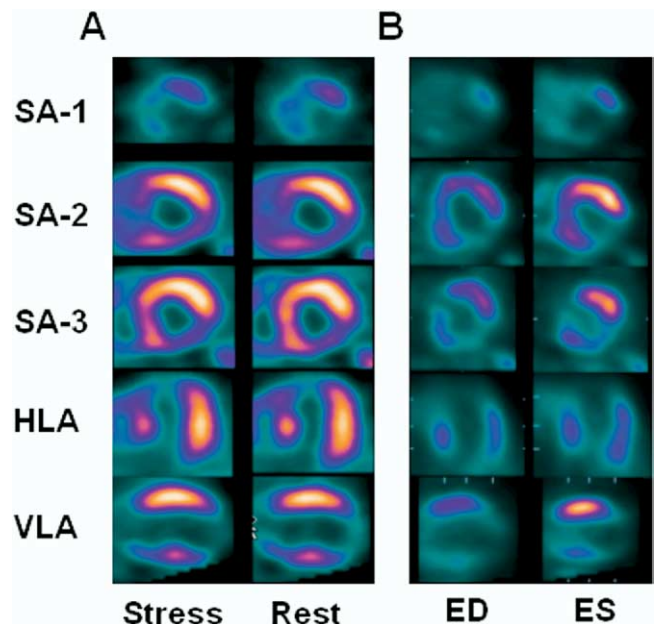
Figure 3 A, Stress and rest of [82]Rb PET images demonstrating severe extensive apical, septal, and inferior scarring and only minimal basal septal ischemia. B, Resting end-diastolic and end-systolic gated images, showing poor or absent contractility in the scarred regions, and poor overall left ventricular function.
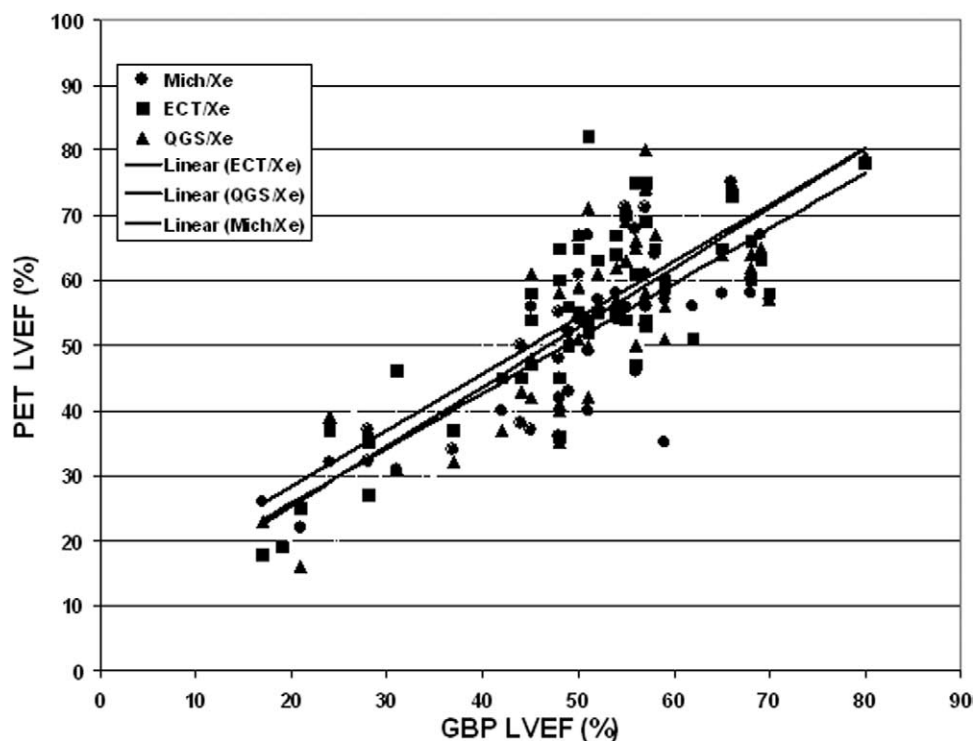
Figure 4 LVEFs obtained from gated ^{82}Rb PET imaging and QGS/Xe, Emory Tool Box (ECT/Xe), and Michigan 4D (MICH/Xe) software, correlated with planar gated blood pool imaging.[236]

have found that filtered back projection with a reconstruction filter and measured attenuation correction produces the best myocardial image uniformity. Iterative reconstruction produced greater regional nonuniformity in normal controls.[43] These results are specific to our PET scanner (AD-VANCE-GE Medical Systems) and should be checked for other scanners. For gated wall motion images, we use iterative reconstruction with segmented attenuation correction to suppress the higher level of noise. The resulting images can be displayed using any of a number of software packages developed for SPECT and adapted for PET.

An important decision is the choice of 2D versus 3D PET imaging, specific for each type of PET scanner. In studies with our bismuth germanate (BGO) crystal scanner, acquisition in 3D mode with high injected doses (50-60 mCi) of ^{82}Rb and immediate acquisition resulted in excessive dead-time and randoms. We obtained good results by delaying acquisition for 5 min after injection, although that defeats the purpose of imaging early in trying to maximize counts. Similar image quality could be obtained with low-dose (20 mCi) ^{82}Rb 3D imaging as with high-dose (50-60 mCi) 2D imaging.[44,45] Our experiments with phantoms showed similar resolution and image quality for 3D and 2D images in lean individuals. In obese individuals, both contrast and image quality were better with 2D imaging. Quantification with 3D imaging should be done with caution, since 3D imaging without proper correction produces significant axial nonuniformity.[46] A clear benefit of 3D imaging with our scanner would be realized if a less expensive low-dose ^{82}Rb generator

were offered. One could then obtain similar results with low-dose 3D imaging as with high dose 2D imaging, at lower cost.

Lutetium orthosilicate (LSO) crystal detector PET scanners (CTI, Knoxville, TN), offer the ability to function in 3D mode at high activities. The cardiac PET laboratory at the Mid America Heart Institute of Kansas City, MO, acquired in quick succession, 2D perfusion and 3D gated imaging at rest and with stress (Table 5). A quantitative comparison[47] between 2D and 3D ^{82}Rb perfusion acquisitions showed the resting images to be identical. 2D and 3D dipyridamole stress images showed significant differences, although follow-up studies showed stress 3D imaging to perform as well as 2D mode imaging in accuracy of perfusion defect detection. Another laboratory observed that compared with a BGO 2D system, an LSO 3D system using a lower 30- to 50-mCi ^{82}Rb dose obtained reduced noise levels, albeit with increased background levels,[48] presumably as the result of a higher randoms level. These observations need to be explored further. Germanium-based 3D scanners also are available (Philips, Cleveland, OH).

With proper image processing, good quality ^{82}Rb PET-gated images can be obtained in the vast majority of patients. Poor gated image quality results from arrhythmia or a slow or fragmented ^{82}Rb injection. We compared visually assessed regional and global left ventricular function from gated ^{82}Rb PET studies to either gated SPECT images or gated planar blood pool images and we demonstrated a 92% agreement in segmental wall motion scores.[49] More recently, we compared the left ventricular ejection fraction (LVEF) calculated with 3
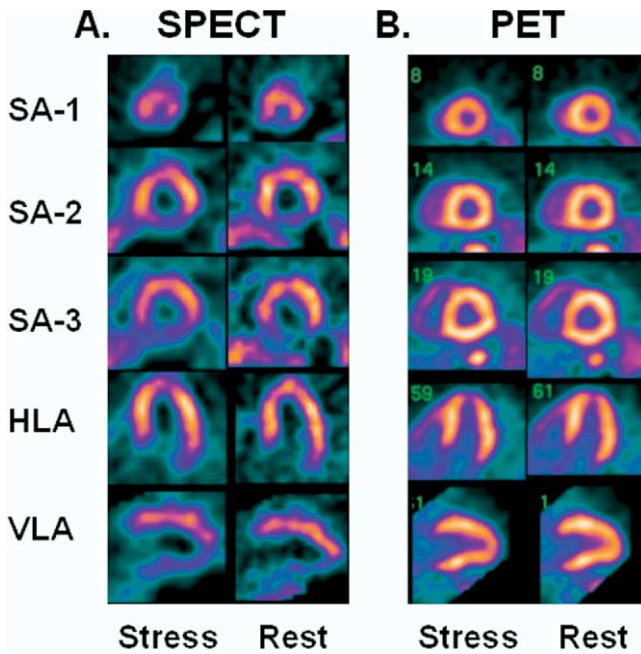
Figure 5 A. Dipyridamole stress and rest ^{99m}Tc sestamibi SPECT images. The stress images show a moderate inferior defect and possible mild anterior defect with mild improvement in the anterior wall and apex at rest. B, The stress and rest PET images showed uniform distribution.

commercial software packages from gated ^{82}Rb PET images to LVEFs obtained from planar gated blood pool images. The results showed all three methods to perform satisfactorily, with correlation coefficients of 0.81 to 0.83[50] (Fig. 4). Another group compared 3D gated ^{82}Rb PET imaging with an LSO system to gated Tc-99 month sestamibi SPECT. The authors found a good correlation ($r = 0.91$) for the LVEFs between the 2 methods.[51] Regional wall motion and LVEFs obtained from ^{13}N ammonia gated PET images also yielded excellent agreement with other wall motion modalities.[52]

The Value of PET for Clinical Imaging

Image Uniformity in PET Imaging

A major challenge for cardiac radionuclide perfusion imaging is nonuniform attenuation of gamma photons in the chest, varying markedly between men and women, and among individuals within each gender. Image uniformity is probably the most important property of cardiac PET perfusion imaging. With coincidence detection, the probability of attenuation for the two gamma photons is uniform along the line between any 2 detectors. This can be measured and corrected. With a conventional gamma camera, resolution deteriorates with distance from the gamma camera, along with attenuation at increasing depth within the subject, which is difficult to model and correct reliably.[53] Although normal maps for SPECT images are nonuniform and different for men and women, the maps with ^{82}Rb PET are uniform and identical for both genders.[54] This is illustrated in Figure 5 for a patient referred for dipyridamole ^{99m}Tc sestamibi SPECT imaging for preoperative risk evaluation. The gated SPECT images showed global hypokinesis. Even though attenuation artifact was suspected, the study could not exclude inferior wall scarring, and possible mild apical and anterior wall ischemia. A short time afterward, stress and rest ^{82}Rb PET images showed uniform distribution. Coronary angiography, performed despite these results, showed normal coronary arteries, with mild diffuse left ventricular dysfunction, probably due to chronic hypertension.

Table 6 lists 8 studies that compared PET myocardial perfusion imaging with angiography, some performed with ^{13}N ammonia and others with ^{82}Rb. Representing a total of 791 patients, they showed a mean 93% sensitivity and 92% specificity for CAD. Table 7 lists studies that compared PET myocardial perfusion imaging with ^{201}Tl SPECT imaging in the same patients. These studies showed higher overall sensitivity, specificity, and accuracy for PET compared with SPECT imaging.

Nondiagnostic or uncertain interpretation of a noninvasive test is one of the factors prompting physicians to recommend further invasive diagnostic studies. In 2748 patients, Patterson and coworkers[55] found a reduction in the number of interpretations classified by 2 experienced physicians as "probably" normal or abnormal, from 37% with ^{201}Tl SPECT, to 21% with ^{82}Rb PET. Regional quantification has been shown to further improve the accuracy of PET perfusion imaging[56,57] with a 99% sensitivity, 83% specificity, and 100% normalcy rate for CAD and a high interobserver agreement of 94% among 3 physicians.[58,59]

During the last 10 to 15 years, both SPECT and PET im-

Table 6 Diagnostic Accuracy of PET Myocardial Perfusion Imaging for CAD

Sensitivity (%)	Specificity (%)	No. Patients	Agent	Author
95	100	50	NH$_3$, ^{82}Rb	Gould et al[224]
94	95	193	^{82}Rb	Demer et al[225]
93	78	202	^{82}Rb	Go et al[226]
97	100	45	NH$_3$	Schelbert et al[227]
93	100	49	NH$_3$	Yonekura et al[228]
98	93	146	^{82}Rb	Williams et al[229]
84	88	81	^{82}Rb	Stewart et al[230]
95	95	25	NH$_3$	Tamaki et al[231]
93	92	791		Average

Table 7 Comparison of PET and SPECT Myocardial Perfusion Imaging for Detection of CAD in the Same Patients

Author	Tracer	Accuracy (%)	Sensitivity (%)	Specificity (%)
Go et al[232] (n = 132)	Rb-82	92	95	82
	T1-201	78	79	76
Stewart et al[233] (n = 81)	Rb-82	85	87	82
	T1-201	78	87	52
Tamaki et al[234] (n = 51)	NH3	98	98	100
	T1-201	98	96	100
Total (n = 264)	PET	91	93	82
	SPECT	81	85	67

aging have undergone significant improvements.[60-65] A recent comparison between Tc-99m sestamibi SPECT and Rb-82 PET myocardial perfusion imaging revealed a significant margin of improvement for CAD detection accuracy with Rb-82 PET compared to SPECT (see Bateman et al[241]). The current literature on the accuracy of PET in comparison with gated attenuation-corrected SPECT is inadequate. Nonetheless, despite ongoing improvements in the accuracy of SPECT, uncertainty remains in many patients even after attenuation correction, with differences in the ability of attenuation correction systems to reduce artifacts.[66]

SPECT imaging in women is challenged by breast attenuation artifact, as well as smaller heart size.[67-69] Williams and coworkers[70] observed a high specificity of stress PET imaging in female patients in relation to coronary angiography. In women who had undergone both stress SPECT and stress PET imaging within a period of 3 months, the SPECT and PET imaging tests had similar high sensitivity, but the specificity for PET was significantly higher than for SPECT. Figure 6 features a 72-year-old female status post heart transplant.
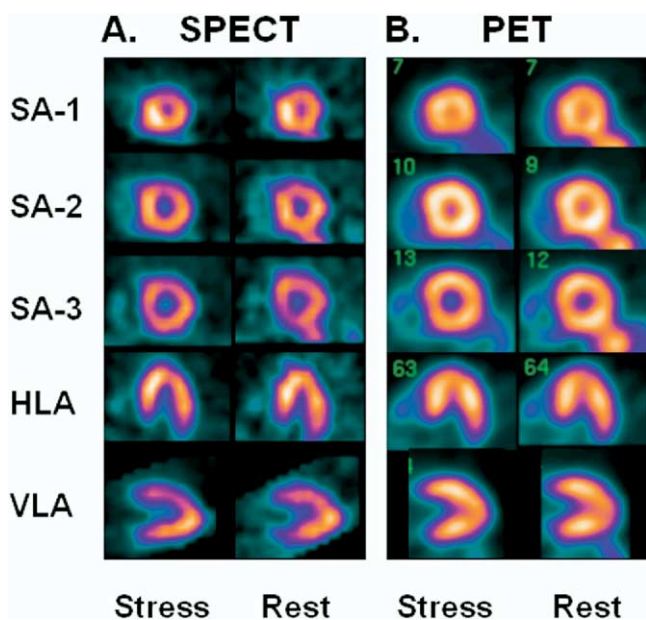
The SPECT images showed a moderate anterior wall defect, with a suggestion of improvement at rest. Even through attenuation artifact was suspected, disease could not be ruled out. The PET imaging study showed normal images. In patients studied with coronary angiography, Patterson and coworkers[71] showed that sensitivity and specificity of CAD detection with PET were equally high for men and women.

An increasing challenge to noninvasive diagnostic imaging is posed by the growing prevalence of moderate and severe obesity in the general population (Table 8). The prevalence of obesity is greater in women, in older individuals, and among African Americans and Hispanic Americans.[72] Obese patients nearly always produce attenuation artifacts on myocardial SPECT perfusion imaging, leading to uncertain results.[73,74] Figure 7 shows SPECT and PET images of a 290-lb, 51-year-old male, with risk factors for CAD. The SPECT attenuation-corrected images show mild to moderate inferior and apical defects which slightly improved on the resting images, accompanied by 1-mm ST depression with nearly maximal exercise. Rb-82 PET images obtained a short time afterward showed a normal distribution. The defects seen on SPECT even after attenuation correction can still be attributed to attenuation.

There are limitations to the ability of PET to image very obese individuals. Most imaging tables are limited to 400- to 450-lb loads. Frequently, the size of the scanner opening is the limiting factor, particularly if it is 60 to 63 cm in diameter. Several currently marketed PET scanners with an opening of 70 cm can be more easily accommodate very large patients.[75]

Imaging in the Pediatric Population

The pediatric population also poses a challenge for diagnostic SPECT imaging. Infants and children can derive benefit from assessment of coronary vessels following switch operations, correction of anomalous coronary arteries (Kawasaki's disease), or in patients with myocardial injuries. Image quality is

Figure 6 A, ^{99m}Tc sestamibi dipyridamole stress and rest SPECT images show a mild-to-moderate anterior wall defect at stress with a suggestion of partial improvement at rest. B, The ^{82}Rb PET imaging study shows normal images.

Table 8 Prevalence of Obesity (BMI >30) in Adults[235]

Year	Men (%)	Women (%)
1960	10.7	15.8
1972	12.1	16.6
1978	12.7	17
1990	20.6	25.9
2000	27.7	34
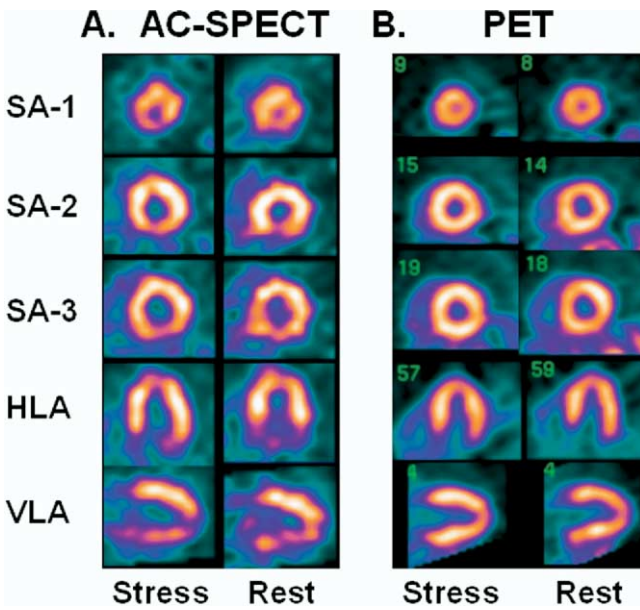
Figure 7 A, Stress and rest attenuation-corrected (AC) ^{99m}Tc sesta-mibi SPECT images of a 290-lb, 51-year-old male. The SPECT image shows mild-to-moderate inferior and apical ischemia and partial scarring. B, The stress and rest PET images showed normal distribution.

limited by poor resolution and low usable activity of ^{201}Tl. ^{99m}Tc sestamibi and ^{99m}Tc tetrofosmin images are compromised by high liver activity in close proximity to the small heart. We have found the results of PET ^{82}Rb myocardial perfusion imaging in infants and in small children to be excellent. The short half-life of ^{82}Rb or ^{13}N ammonia allows sufficiently high doses of tracer to be delivered to achieve good quality images with low radiation exposure to the child.

Prognostic Value of Myocardial PET Imaging

Given the proven value of PET myocardial perfusion imaging in the diagnosis of CAD, it is expected that the prognostic value of gated PET is also high, similar to SPECT imaging. In 153 patients studied with ^{82}Rb PET imaging, Yoshinaga and coworkers showed 94% event-free survival during a 3-year period in patients with normal PET scans, compared with 62% with mild defects, 58% with moderate defects, and 45% survival with severe defects.[76] VanTosh and coworkers[77] showed that a normal stress PET study in women with chest pain and significant cardiac risk factors predicts a very low cardiac event rate.

Detection of Diffuse and Early Disease

PET imaging appears to be useful in the diagnosis and prognostication at an early stage in disease and in the measurement of the response to dietary and lifestyle changes and antilipid drug therapy.[78,79] Merhige and coworkers[80] studied 128 patients with CAD with stress and rest ^{82}Rb PET. After aggressive lipid-lowering therapy, 80 patients demonstrated improvement in myocardial perfusion, 64 patients showed

no change, and 34 showed progression of CAD despite treatment at a mean follow-up of 1.5 years. Then, 7.5 months after the second scan, coronary events had occurred in 3.3%, 10.9%, and 17.7% of patients, respectively. Thus, PET perfusion imaging identified 26% of patients with progressive CAD, despite lipid lowering therapy, at a high-risk of subsequent hard coronary events.

Base to Apex Flow Gradient Quantification

Invasive studies with Doppler flow and pressure probes have demonstrated a continuous gradient between the proximal and distal portions of coronary arteries with diffuse, though nonobstructive disease, resulting in a gradient in flow reserve.[82] In such patients, once attenuation correction has been successfully applied, Gould and coworkers demonstrated with PET a graded, longitudinal, base-to-apex myocardial perfusion gradient significantly different from normal control subjects (Fig. 8).[82] This observation was confirmed by Pampaloni and coworkers.[83] An abnormal base-to-apex perfusion gradient observed during vasodilator stress suggests the presence of early or preclinical CAD.
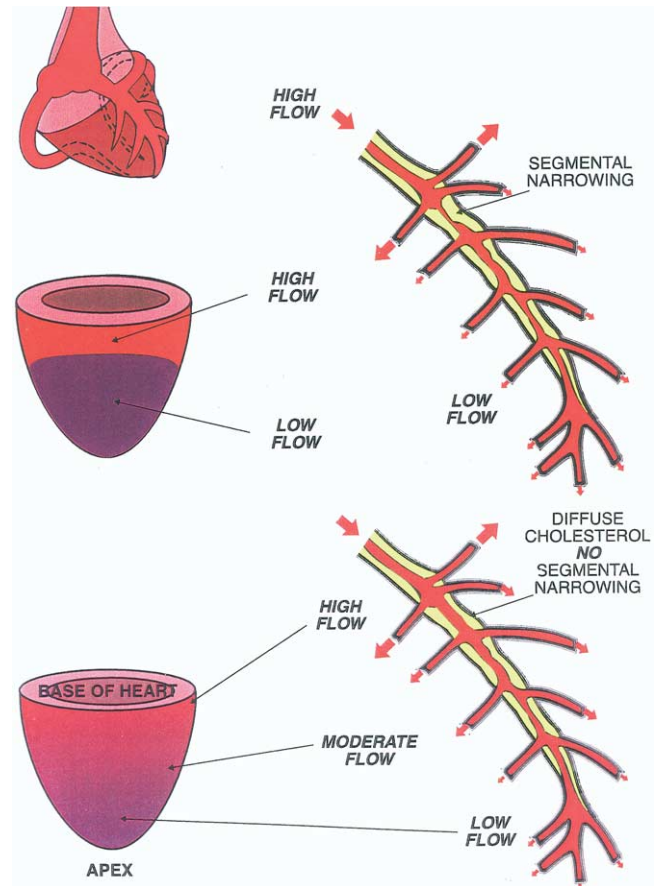
Figure 8 Schema of a longitudinal base-to-apex myocardial perfusion abnormality caused by diffuse coronary artery narrowing compared with segmental perfusion defects caused by localized stenosis. (Reproduced with permission from Gould et al.[82])

Table 9 Clinical Applications of Coronary Flow Reserve Quantification

1. Verification of efficacy of pharmacological vasodilation
2. Detection of global/diffuse disease
3. Evaluation of extent of multivessel disease
4. Evaluation of significance of individual vessel lesions
5. Detection of coronary steal syndrome-collaterals
6. Evaluation of endothelial function
7. Monitoring therapy

Quantification of Myocardial Blood Flow

The noninvasive quantification of myocardial blood flow and coronary flow reserve is one of the most potentially useful but as yet clinically unrealized applications of myocardial PET imaging. Formal quantification of blood flow usually requires a multi-frame (50 frames or so) dynamic PET acquisition. Myocardial and blood-pool activity curves are generated and corrected for decay, partial volume effect, and tissue cross-talk. A compartmental model is then applied to solve for blood flow.

The rapid equilibration of ^{15}O water between plasma, interstitial space, and intracellular water allows the use of a simple 1-compartment model,[84] making this tracer a favorite in scientific studies of quantitative myocardial perfusion. ^{15}O water is not a very useful clinical perfusion imaging agent because of its poor image quality and a requirement for a cyclotron. ^{13}N ammonia has been used for blood flow measurements in many pioneering studies of myocardial vascular pathophysiology.[85] With the use of a 2-compartmental model, satisfactory reproducibility and accuracy are obtainable.[86,87] Quantification of blood flow with ^{82}Rb is possible as well. Because of its 75-s half-life, myocardial and blood pool time-activity curves are noisy. Compartmental analysis of ^{82}Rb in humans has yielded a fair reproducibility in our laboratory ($r = 0.83$).[88] Lin and coworkers demonstrated that with specialized wavelet-based noise reduction methods, the correlation between ^{82}Rb flow with ^{15}O water flow was excellent ($r = 0.94$).[89]

Limitations of compartmental modeling include the need for a multiframe dynamic acquisition, requirement for high expertise, and the fact that it is time-consuming. It is likely that standardized acquisition protocols and commercial development of analysis software will make this important PET capability accessible for routine use.

It is possible to estimate blood flow and coronary flow reserve using methods which, although lacking the rigor of compartmental analysis, offer greater simplicity and ease of use. The simplest approach uses the ratio of ^{82}Rb uptake during stress and during rest after normalization for injected activity. The uptake ratio reflects coronary flow reserve, although it ignores the effects of cardiac output on the plasma tracer activity and decreasing extraction fraction of ^{82}Rb during hyperemia. The stress/rest ^{82}Rb uptake ratio has been used successfully as an index of blood flow response to stress the presence of left ventricular hypertrophy and in the detection of coronary steal syndrome.[90-92]

A compromise alternative proposed by Yoshida and co-

workers[93] corrects the uptake of ^{82}Rb or ^{13}N ammonia by the summed blood pool activity and by the relation between the extraction fraction and blood flow obtained from animal experiments.[94,95] This approach (simple model) was validated in animal experiments. We have adapted this method for human studies. A comparison of the simple model with the compartmental model yielded a fair correlation ($r = 0.72$, $P < 0.001$), and excellent reproducibility ($r = 0.97$), less susceptible to noise than the compartmental method.[96] Using a similar method of measuring ^{82}Rb retention, DeKemp and coworkers showed a good reproducibility and good correlation with microsphere flow measurements ($r = 0.74$; $P = 0.001$) in animal studies.[97]

Clinical Applications of Myocardial Blood Flow and Coronary Flow Reserve

Some clinical applications of coronary flow reserve (CFR) are listed in Table 9. The first application is quality control to verify the global response to vasodilator stress. A normal flow reserve (greater than 2.0 in our normal population), provides assurance that the stress test was adequate. In patients with decreased flow reserve, ie, patients who ingested some caffeine, those who have small vessel disease because of hypertension or diabetes or endothelial dysfunction because of hyperlipidemia or diabetes,[98,99] or patients with end-stage liver disease,[100,101] the sensitivity of conventional imaging to detect epicardial coronary disease may be limited. In the absence of flow reserve quantification, the adequacy of response to pharmacological stress is unknown.[102]

Another important application is to help detect extensive epicardial disease in a high-risk patient with normal or minimally abnormal stress and rest images due to "balanced ischemia." Figure 9 shows stress and rest images of a 70-year-old male with multiple risk factors for CAD and mild chest pain.
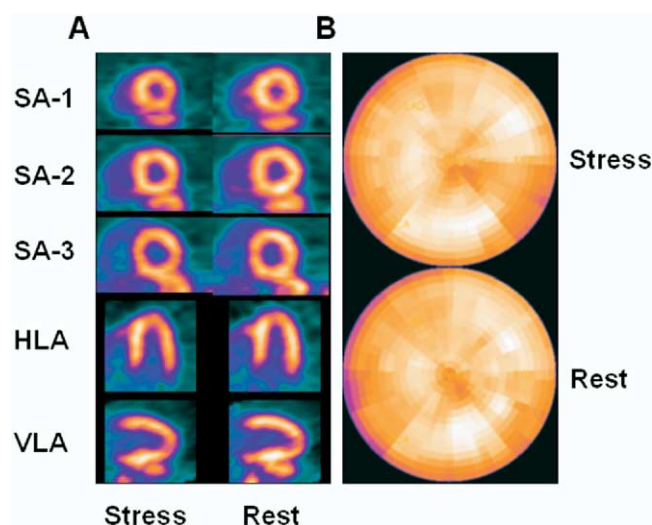
Figure 9 Tomographic slices (A) and the polar maps (B) of stress and rest ^{82}Rb PET images of a 70-year-old male with multiple risk factors for CAD and mild chest pain. The images suggest only minimal apical and inferolateral ischemia. The CFR was 1.3, indicating severe diffuse disease.

During dipyridamole stress, the ECG response was negative, and the stress ^{82}Rb PET images showed only minimal apical and inferolateral ischemia. This would not necessarily be a patient for invasive evaluation, were it not for the fact that the global CFR was only 1.3 (normal CFR >2.0). The patient's angiogram showed 3-vessel disease, which was deemed most severe in the OM1 branch of the left circumflex artery. Quantification of coronary flow reserve has recently been shown to improve differenciation between 3-vessel and 1-vessel disease. Flow reserve quantification thus helps define the full extent of multi-vessel disease,[103] by assessing disease severity not only in the abnormal segments but also in the "normal" segments, when these "normal" segments are used for normalization of stress and rest images.

Coronary arteriography is considered the "gold standard" for evaluating the severity of coronary stenosis. Muzik and coworkers found a high diagnostic accuracy and sensitivity using absolute ^{13}N ammonia blood flow for the detection of coronary disease. In patients with a low probability of CAD, the specificity was also high, whereas an abnormal flow reserve in regions with angiographically normal territories in patients with CAD elsewhere was postulated to represent early functional vascular abnormality.[104] Because the resistance to blood flow through a stenotic lesion depends on a number of lesion characteristics, the physiologic significance of coronary lesions of intermediate severity often is difficult to determine from angiography alone.[105-108] Multiple factors other than lesion diameter influence the measured coronary flow reserve, including the heart rate, resting blood flow, the left-ventricular end-diastolic pressure, contractility, and the magnitude of dipyridamole-induced hyperemia,[109-112] Nevertheless, there is a role for the accurate assessment of the physiologic severity of coronary stenoses as a more objective determination of medical versus mechanical treatment of coronary artery stenosis and for monitoring of the results of their treatment, since clinical tools, such as chest pain, are poorly related to stenosis severity.

Another application of occasional usefulness in intervention is the assessment of collaterals in diseased regions. It is axiomatic that blood flow in diseased arteries does not increase to the same degree as in normal vessels. In multivessel disease, in regions supplied by collaterals, blood flow may actually decrease with stress, demonstrating "coronary steal," which can be detected by quantification of regional blood flow.[113-115] Knowledge of such collaterals, which can't always be seen angiographically, can help in the planning of high-risk intervention procedures.

Another application is the monitoring of the progression or possible regression of diffuse disease in atherosclerosis, hypertension, diabetes, hyperlipidemia, and posttransplant vasculopathy.[116-118] The patient shown in Figure 9 declined CABG and allowed the revascularization of only the OM1, the most severely diseased vessel. The patient was placed on a rigorous antilipid regimen with diet and medication. One year later, the PET study was repeated. The study did not show any focal abnormality, and the global CFR was 2.2 (normal), and at 2 years, the CFR was 2.9, demonstrating reversibility of the hemodynamic effects of CAD with diet and antilipid medication alone, a phenomenon documented in the literature.[119-121]

Detection of Early Disease

Decreased CFR has been found even in the absence of coronary stenoses, in normal-appearing vessels in patients with coronary disease in other vessels.[122-124] The presence of even mild, nonobstructive coronary disease was found to be predictive of progression to clinically significant disease in 6 years.[125] Quantitative PET offers a sensitive tool to detect early disease in high risk asymptomatic individuals with family history of CAD.[127] CFR has been shown to be decreased in hypertrophic disease states,[127] in poorly controlled diabetes or hyperlipidemia.[128-130] Glycemic control and reduction of serum lipids through low-fat diet, exercise and antilipid drugs have been shown to lead to improvements in CFR.[131,132]

Cold Pressor Stress Testing. The vascular endothelium plays an important role in the regulation of circulatory function and in the structural and functional integrity of the vascular wall.[133] Intracoronary acetylcholine normally causes endothelial release of nitric oxide (NO) and vasodilation. In the presence of endothelial disease, acetylcholine produces lack of vasodilation, or even vasoconstriction. Abnormal endothelium-dependent coronary vasomotion has been found to be an independent predictor of coronary artery disease and of coronary events.[134-136] Normal response has been restored after cholesterol lowering and antioxidant therapy.[137]

Endothelial function also can be studied with flow-dependent vasodilation in response to cold-pressor testing (CPT).[138] CPT consists of immersing one hand in ice or ice water for 60 s before the injection of a flow tracer and for 60 s after the injection. CPT results in sympathetic stimulation[139] and alpha-adrenergic mediated vasoconstriction of vascular smooth muscles, which is, under normal conditions, offset by flow-mediated vasodilation and a possible direct adrenergic-induced endothelium-dependent vasodilator response.[140] In the presence of endothelial disease or atherosclerosis, the vasoconstrictor component is left unopposed.[141,142] Changes in luminal area of the epicardial vessels during CPT correlate with changes in coronary blood flow, demonstrating that flow-dependent vasodilation can be studied with measurements of coronary blood flow.[143,144] A 30% to 40% increase in blood flow is considered a normal response to CPT. Despite angiographically normal coronary arteries, a diminished or even paradoxically decreased endothelium-dependent flow response may result in a mismatch between demand and supply, that has been related to myocardial ischemia during daily life.[145-147] An example is given by a 58-year-old female with hyperlipidemia and chest pain, who was initially diagnosed with a distal LAD artery occlusion, which was treated with a stent. After several years of doing well, the patient presented with atypical chest pains at night and in cold weather. An angiogram showed no obstructive disease. The patient underwent serial imaging at rest, CPT, and adenosine stress testing with Rb-82 PET
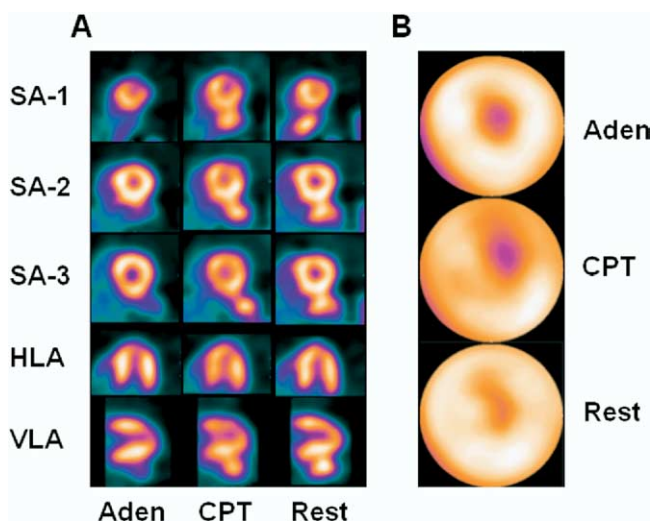
Figure 10 [82]Rb PET tomographic images (A) and polar maps (B) of adenosine stress, CPT, and resting images of a 58-year-old female with atypical chest pains at night and in cold weather but no obstructive coronary disease. Resting perfusion is normal. The adenosine stress images show mild anteroapical hypoperfusion. The cold-pressor perfusion images show moderate anteroapical and extensive mild anterior, anterolateral, and septal hypopoperfusion.

imaging. The results are shown in Figure 10. The resting images are normal. The adenosine stress images show mild anteroapical hypoperfusion suggestive of a base-to-apex flow gradient, as proposed in Figure 8. The cold-pressor images show moderate anteroapical and extensive mild anterior, anterolateral, and septal hypopoperfusion accompanied by her usual chest pain. The patient was given a calcium channel blocker, and more aggressive antilipid therapy with complete relief of symptoms.

Abnormal responses to CPT have been found in early coronary artery disease,[148] hyperlipidemia,[149,150] insulin resistance,[151] diabetes,[152,153] elevated CRP levels,[154] the metabolic syndrome,[155] elevated leptin levels in obese individuals,[156] and smoking.[157,158] Endothelial dysfunction is reversible with insulin-sensitizing drugs in the case of insulin resistance, improved glycemic control or ACE inhibitors in diabetes, L-arginine, citric acid or smoking cessation in smokers, and antilipid therapy in patients with elevated serum lipids.[159-162] Abnormal CPT results have been associated with menopause,[162] that can be reversed by long-term hormone replacement therapy.[163]

The response to CPT is more dramatic compared with the minimal changes in angiographic CAD lesion characteristics or lumen diameter[164] and tends to be more sensitive than the response to hyperemia (dipyridamole or adenosine).[165] The fact that some patients with risk factors have a normal response to CPT, whereas others have an abnormal response, or that some "normal" subjects may have an abnormal response,[166] attest to the variability of the susceptibility of the individual. Of relevance is the observation that only 50% of the total attributable risk burden for CAD can be related to conventional risk factors,[167,168] warranting an alternative determination of risk

for the development of atherosclerosis. Noninvasive CPT can serve as an early marker of endothelial dysfunction, and development of atherosclerosis, that is susceptible to reversibility with diet and medication.[169]

Is Myocardial PET Perfusion Imaging Cost-Effective?

The use of PET perfusion imaging has been shown to be cost-effective through its enhanced diagnostic power. The results of an analysis by Gould and coworkers[170-172] are shown in Figure 11. The most expensive diagnostic approach is that of coronary angiography in all patients with a pretest probability of less than 70%. In patients with a greater than 70% likelihood of disease, angiography is more cost-effective for diagnosis. Both SPECT and PET achieve a savings compared with performing angiography, due to deceased referral for unnecessary coronary catheterization. PET achieves a savings compared with SPECT for patients with a probability of disease between 0 and 60. If only half of patients with an abnormal noninvasive test undergo angiography, then the cost savings of PET is even greater. A cost analysis by Patterson and coworkers[173] came to similar conclusions.

Merhige[174] studied what actually happens when PET imaging is introduced into clinical practice. 102 patients studied with stress-rest [82]Rb PET imaging were identified, with a mean pretest probability for CAD of 37% were compared with 102 matched patients tested with SPECT. After a follow-up of 12 months, the use of PET led to a reduction in the false positive rate resulting in a reduction in angiographies. While there was no significant change in the rate of angioplasties, there was a reduction in the number of bypass operations. The diagnostic cost per patient was similar for SPECT and PET, despite higher cost of PET per study, due to lower referral for further diagnostic studies. The therapeutic
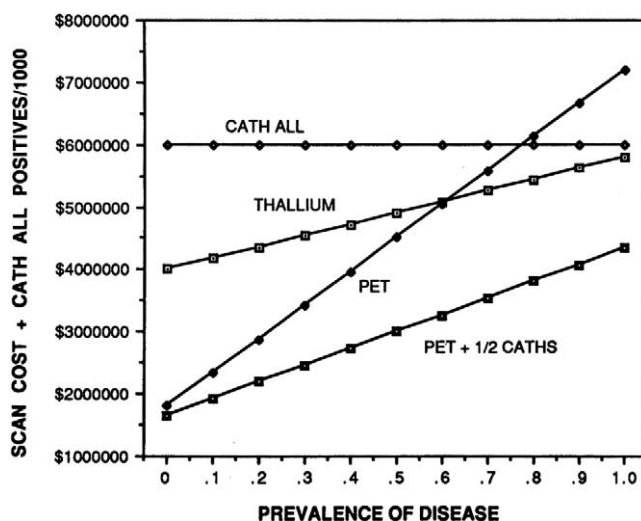
Figure 11 Comparative costs of ^{201}Tl SPECT, [82]Rb PET, and coronary angiography as a function of disease prevalence. (Reprinted by permission of the Society of Nuclear Medicine.[238])

cost per patient was lower with PET, attributable to a reduction in the number of bypass operations, as predicted by Patterson and coworkers.[175]

Myocardial Viability

Why PET Viability Imaging Matters

Viability imaging is reviewed separately in this seminar. The consideration of myocardial viability is important in a patient with impaired left ventricular function because of coronary artery disease with a possibility of revascularization. Flow measurements in these dysfunctional regions by SPECT or PET perfusion imaging, particularly those with mild-to-moderate flow reduction do not by themselves distinguish between regions with potentially reversible dysfunction and regions with irreversible dysfunction.[176] Combined metabolic and perfusion PET imaging offers diagnostic power in the prediction of myocardial functional recovery of viable myocardium.

It also has high prognostic power in predicting symptomatic improvement in patients with congestive heart failure[177] and predicting high level of cardiac events in patients with poor left ventricular function in the presence of significant areas of perfusion-metabolism mismatch treated medically, and lower event rate in patients undergoing revascularization.[178-183]

The clinical value of cardiac FDG-PET imaging in the assessment of myocardial viability in combination with perfusion imaging was demonstrated more than 18 years ago.[184] In direct comparison between thallium-201 SPECT or ^{99m}Tc Sestamibi with FDG imaging in the same patients with very poor left ventricular function, FDG-PET imaging showed incremental benefit over thalium-201 stress-redistribution /reinjection or ^{99m}Tc sestamibi SPECT imaging in predicting functional recovery, while in patients with relatively preserved left ventricular function, the predictive value was similar.[185,186] PET viability imaging also has been successfully applied in infants and children with high accuracy, similar to that seen in adults.[187]

In our protocol, the patient undergoes resting perfusion imaging with ^{82}Rb and, whenever possible, pharmacologic stress ^{82}Rb perfusion imaging. This is followed by FDG-PET imaging, which begins with glucose loading and supplementary insulin.[188] The patient is injected with FDG. After a 1-h rest, the patient then undergoes emission PET imaging, along with a transmission scan.

Because ^{82}Rb is an analog of ^{201}Tl, it is not surprising that ^{82}Rb often shows reversible stress-rest defect, whereas ^{99m}Tc sestamibi or ^{99m}Tc tetrofosmin SPECT studies show extensive fixed defects.[189] Nevertheless, FDG-PET imaging frequently shows additional viability in patients with fixed ^{82}Rb perfusion defects or in patients with only partial stress-inducible reversibility. An example is a 49-year-old male with a history of myocardial infarction, very poor left ventricular function, and congestive heart failure. Exercise stress ^{99m}Tc MIBI images (Fig. 12) showed severe apical, anterior, lateral, and inferior defects, with no improvement on the rest images.
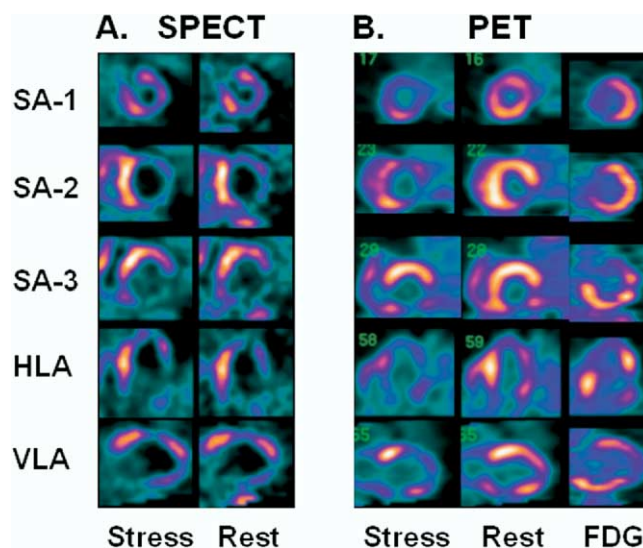
Figure 12 A, ^{99m}Tc sestamibi (MIBI) exercise stress and rest images in a 49-year-old male with known CAD and congestive heart failure. The MIBI images show severe apical, anterior, lateral, and inferior defects with no improvement on the resting images. B, The dipyridamole stress ^{82}Rb images show severe apical, anterior, lateral and inferior-basal defects, and a moderate-to-severe septal defect. The resting ^{82}Rb images show marked anterior, septal and anterolateral improvement, and mid-inferior improvement. The FDG-PET images showed preserved or increased activity in the anterolateral, lateral, inferior and inferior-basal walls, demonstrating a classical mismatch pattern in these regions.

Dipyridamole stress ^{82}Rb images showed severe apical, anterior, lateral, and inferior defects, and a moderate to severe septal defect. The resting images, however, showed marked anterior, septal and anterolateral improvement, and inferior improvement. The extent of stress-inducible ischemia was at least 50% of the myocardium. In addition, the FDG PET images showed preserved or increased activity in the anterolateral, lateral, inferior and posterior walls, demonstrating a classical mismatch pattern in these regions, occupying at least 50% of the myocardium. About 75% of the myocardial mass showed either stress-inducible ischemia or hibernation, including most of the regions considered scarred by MIBI SPECT imaging. In some instances, it is not necessary to proceed with FDG PET viability imaging, if the stress and rest ^{82}Rb PET imaging provides evidence of ischemia, rather than scarring.

Studies of PET Perfusion Tracer Kinetics for Viability

Because ^{82}Rb is an analog of ^{201}Tl, an attempt was made to analyze myocardial kinetics with ^{82}Rb. Despite the short half-life of ^{82}Rb, animal studies showed that acutely injured, post-ischemic myocardium that eventually proved to be viable showed retention of ^{82}Rb, whereas myocardium, which proved to be necrotic, showed washout of ^{82}Rb.[190] This was supported by clinical studies that measured the washout rate between 1 to 2 min after injection versus 4 to 6 min afterward (Fig. 13) and compared uptake and retention of ^{82}Rb in com-
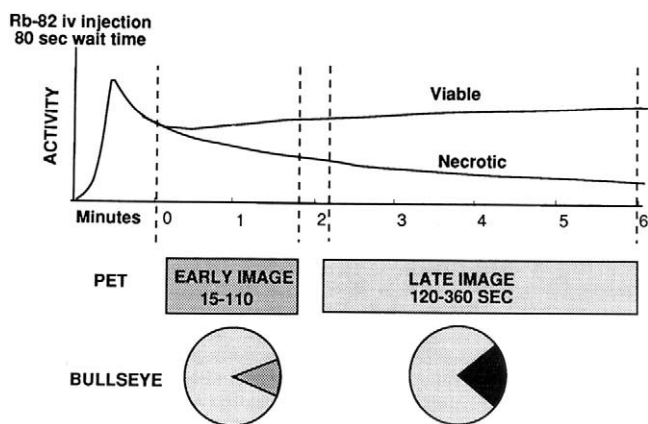
Figure 13 Schematic of the imaging protocol utilizing washout or retention of Rb-82 for assessing myocardial viability. (Reprinted by permission of the Society of Nuclear Medicine.[239])

parison to FDG-PET imaging studies.[191,192] Another study found a significant difference in [82]Rb kinetics between metabolically active and irreversibly injured myocardium.[193] We found a greater [82]Rb washout rate with increasing severity of defects, regardless of the FDG uptake.[194] This issue remains open to further studies.

Beanlands and coworkers[195] studied the ability of ^{13}N ammonia kinetic modeling to calculate viability and compared the results with ^{18}F FDG uptake. Flow and the volume of distribution were both reduced in the hypoperfused regions of patients with scar, whereas partially preserved flow and volume of distribution were seen in regions with viability. The sensitivity and specificity of this combination were 100% and 90%, respectively. These interesting results deserve further studies.

Technical Problems Encountered With Cardiac PET Imaging

The vast majority of patients tolerate PET imaging well. Occasional patients do feel claustrophobic. Patients should be offered sedation in that event. Frequently, a thorough explanation of the procedure, providing reassurance, soothing or favorite music, and close supervision can overcome this difficulty without medication.

Myocardial PET imaging is subject to artifacts. A faulty detector block can cause a major streak and defect artifact. Recognition and checking the PET blank study aids in diagnosing the problem. The assumption of successful PET attenuation correction is that the transmission scan reflects the true position of the heart, diaphragm and adjacent structures. Significant displacement of the average position of the heart due to hyperventilation during stress or a change in respiratory pattern after falling asleep will violate that assumption and leads to artifact.

Our recent work with 178 patients studied with dipyridamole stress and rest [82]Rb PET imaging[196] showed that prevalence of noticeable vertical heart movement of more than 10 mm was 6% in an unselected group of 100 patients, 17% in a subset of 78 asymptomatic patients, and 14% in a subset of 27 patients at low risk of CAD. Despite that, there was no significant increase in frequency of PET scan defects with large or small heart drop in any of patient subgroups, including in the group with low probability of CAD. Fortunately motion does not always lead to artifactual findings, but should be suspected in cases of basal anterolateral, anteroseptal or lateral defects in the presence of excessive displacement.

Analysis of artifacts in PET perfusion images due to transmission-emission misregistration was recently published by Loghin and coworkers,[197] who performed 1177 studies with either [82]Rb or ^{13}N ammonia, while varying the order of transmission and emission scans. They found that 21% of subjects had artifactual defects due to transmission-emission misregistration. Misregistration defects were predicted by horizontal plane misregistration, which was predicted by diaphragm displacement between rest and dipyridamole stress images, a greater body mass index, and small heart size. Misregistration was greatest with transmission scans performed early in the imaging protocol. This was predictably greater in obese individuals, suggesting delayed displacement of the diaphragm after positioning due to pressure from abdominal contents. By shifting the emission images to match the transmission scan during postprocessing, the quantitative severity and size of defects was significantly decreased.

This problem needs appropriate software to display superimposed emission and transmission scans, timely visual or automatic recognition of misregistration movement, both in plane and between transaxial planes, and taking corrective measures. When feasible, a separate transmission scan with each of the resting and stress studies used in some laboratories is a useful step (Table 5). In our protocol (Table 4), we perform the transmission scan after the resting scans, just before the pharmacological stress, thus close in time to both rest and stress imaging. This may account for the relatively lower frequency of displacement misregistration artifact in our studies.[198]

Impact of PET-Computed Tomography (CT)

Combined PET and CT imaging in a single combined PET-CT unit has become the preferred approach for PET imaging in oncology. Approximately 80% new PET units installed in 2003 were PET-CT units (GE Medical Systems, personal communication, 2004). Table 10 summarizes the potential benefits of PET-CT in cardiac imaging. First, the scout CT scan can, in a few seconds, check the proper positioning of the patient. The CT transmission scan lasting 15 to 30 s reduces imaging time. The time savings is not only the time needed for the pin-source transmission scan, but because the CT transmission scan is relatively free of noise, it reduces the amount of noise in the attenuation-corrected emission scan, thereby reducing the length of time required for the emission scan itself. One group reported saving 12

Table 10 Value of PET-CT

1. Positioning
2. Attenuation correction
3. Calcium scoring
4. Coronary angiography
5. Contrast ventriculography

min per study after switching from a dedicated PET system to a PET-CT system.[199] Because 30 to 35 min are required for the entire study, with possibly 45 minutes for the more difficult patients,[200] throughput should be enhanced.

PET-CT imaging holds both challenges and solutions for the attenuation correction problem. It is possible to repeat the CT transmission scan separately for both rest and stress images.[201] The CT transmission and PET emission scans can be easily displayed using existing display software. The CT transmission map can be potentially moved to provide more reliable attenuation correction.

CT attenuation correction also is more susceptible to artifacts produced by metallic implants or pacemakers, than pin source-produced attenuation maps. A very short scanning time for the CT attenuation map may under-sample the position of the heart and diaphragm, due to cardiac contraction, and respiratory movement,[202] seen frequently in whole body PET imaging for oncology purposes.[203] The transmission scan needs to be obtained over a sufficient number of respiratory and cardiac cycles, to match the average position of the heart during the emission scan at rest and again during stress.[204] The radiograph tube current used for the transmission scan needs to be low, to minimize radiation exposure. Such an approach has been taken at the Brigham and Women's Medical Center (Table 11). The most optimal protocol for PET-CT has not yet been determined, due to the limited experience with PET-CT imaging of the heart. Respiratory gating of the CT as well as the PET images offers the potential for a closer emission-transmission match.[205-207] It is hoped that PET camera manufacturers will address this important need.

Another potential application of PET-CT is the possibility of obtaining coronary calcium scores at the same imaging session as the PET scan, which is feasible with an 8- or 16-slice multidetector CT scanner. Calcium scoring requires a higher current from the CT radiograph tube than the transmission scan, resulting in higher patient radiation exposure, but still lower than for CT diagnostic imaging. The clinical value of coronary calcium scoring is at this time still an open question in clinical practice. In patients with risk factors but few symptoms being screened for CAD, calcium scoring can add specificity when the calcium score is low and the perfusion results are equivocal or abnormal due to endothelial dysfunction. The calcium score can add sensitivity in the detection of preclinical CAD, even in the presence of normal myocardial perfusion. Facta and coworkers[208] found that the presence of calcium is associated with mild functional alteration of coronary circulation in apparently healthy individuals, whereas in type 2 diabetic patients, coronary vasomotion abnormalities were independent of epicardial calcifications.

By contrast, Prior and coworkers[209] found that the flow response to CPT or adenosine did not correlate with calcium scores. Glass and coworkers[210] found that the presence, location, and severity of myocardial perfusion defects or angiographic lesions did not correlate with global calcium scores. Thus, regional coronary disease and calcium deposition provide different information. Their interaction and significance needs to be explored.

An intriguing possibility is the potential value of CT coronary angiography performed together with PET rest and stress and/or viability imaging in selected patients. Multislice (16 slices or greater) CT scans have been found to have sufficient temporal resolution to image, with intravenous contrast, coronary arteries with a diameter or 1.5 mm or greater, with a reported sensitivity for 50% or greater coronary lesions of 86% to 92%, a specificity of 93% to 99%, and accuracy of 93% compared with invasive coronary angiography.[211,212] There are limitations in visualizing lesions in the smallest distal vessels, and in the presence of heavy calcifications. The latter limitation can be overcome with the aid of the PET perfusion results.[213]

It is conceivable that patients with known or suspected disease could be studied with sequential stress-rest perfusion imaging and CT angiography and ventriculography, allowing acquisitions of superimposed images of both coronary anatomy, perfusion, wall motion, and viability.[214] This complete set of spatially mapped information could add precision and ease to decision-making for interventions in multivessel disease intervention planning, or in patients with physiologically abnormal perfusion but anatomically normal coronary arteries. This proposition still needs to be tested in clinical studies.

Future Prospects

The extensive infrastructure of PET scanners, availability of perfusion and viability tracers and reimbursement have set the stage for more widespread use of PET for indications shown to be of benefit. In the meantime, there have been several major paradigm shifts in the understanding and management of coronary disease, in which PET imaging of the heart is well suited to play a role. One is the shift in emphasis from the assessment of structural to functional alterations. With quantification of myocardial blood flow, PET can detect

Table 11 Imaging Protocol for [82]Rb PET Imaging With a PET–CT Scanner[234]

Procedure	Time
Positioning (Scout)	1 min
CT transmission scan	1 min
Rest gated imaging	8 min
Rest perfusion imaging	8 min
Pharmacological stress	7 min
CT transmission scan	
Stress imaging	8 min
Total duration	33 min

early endothelial disease in the absence of obstructive disease, which is predictive of future development of disease, even in patients that lack classical risk factors, and which can be reversed by lifestyle, dietary, and pharmacologic interventions. Thus, the study of endothelial dysfunction is suggested to be a key to the early diagnosis and control of early coronary disease. Another unique feature of PET is the ability to image as yet nonroutine tracers labeled with isotopes like ^{18}F, ^{11}C, and [13]N. Finally, a major paradigm shift is offered by the intriguing potential of combined multimodality imaging, represented by PET-CT imaging. The growing PET infrastructure is allowing PET imaging to become a tool in the noninvasive assessment of in vivo cellular metabolism, receptor function and gene expression, which hold great potential in applications beyond perfusion and glucose metabolism discussed in this review.

Acknowledgments

References

1. Kong BA, Shaw LS, Miller DD, et al: Comparison of accuracy for detecting coronary artery disease and side-effect profile of dipyridamole thallium-201 myocardial perfusion imaging in women versus men. Am J Cardiol 70:168-173, 1992

2. Nishimura S, Mahmarian JJ, Boyce TM, et al: Quantitative thallium-201 single-photon emission computed tomography during maximal pharmacologic coronary vasodilation with adenosine for assessing coronary artery disease. J Am Coll Cardiol 18:736-745, 1991

3. Bateman TM, Maddahi J, Gray RJ, et al: Diffuse slow washout of myocardial thallium-201: a new scintigraphic indicator of extensive coronary artery disease. J Am Coll Cardiol 4:55-64, 1984

4. Aarnoudse WH, Botman KJ, Pijls NH: False-negative myocardial scintigraphy in balanced three-vessel disease, revealed by coronary pressure measurement. Int J Cardiovasc Intervent 5:67-71, 2003

5. Stolzenberg J: Dilataiton of left ventricular cavity on stress thallium scan as an indicator of ischemic disease. Clin Nucl Med 5:289-291, 1980

6. Kumar SP, Movahed A: Importance of wall motion analysis in the diagnosis of left main disease using stress nuclear myocardial perfusion imaging. Int J Cardiovasc Imaging 19:219-224, 2003.

7. Martin W, Tweddel AC, Hutton I: Balanced triple-vessel disease: enhanced detection by estimated myocardial thallium uptake. Nucl Med Commun 13:149-153, 1992

8. Falk E, Shah PK, Fuster V: Coronary plaque disruption. Circulation 92:657-671, 1995

9. Libby P: Molecular bases of the acute coronary syndromes. Circulation 91:2844-2850, 1995

10. Farb A, Tang AL, Burke AP, et al: Sudden coronary death: frequency of active coronary lesions, inactive coronary lesions, and myocardial infarction. Circulation 92:1701-1709, 1995

11. Gould KL, Martucci JP, Goldberg DI, et al: Short-term cholesterol lowering decreases in size and severity of perfusion abnormalities by positron emission tomography after dipyridamole in patients with coronary artery disease. Circulation 89:1530-1538, 1994

12. Gould K, Ornish D, Scherwitz L, et al: Changes in myocardial perfusion abnormalities by positron emission tomography after long-term, intense risk factor modification. JAMA 274:894-901, 1995

13. Czernin J, Barnard RJ, Sun KT, et al: Effect of short-term cardiovascular conditioning and low-fat diet diet on myocardial blood flow and flow reserve. Circulation 92:197-204, 1995

14. Yokoyama I, Momomura S, Ohtake T, et al: Improvement of impaired myocardial vasodilation due to diffuse coronary sclerosis in hypercholesterolemics after lipid-lowering therapy. Circulation 100:117-122, 1999

15. Huggins GS, Pasternak RC, Alpert NM, et al: Effects of short-term treatment of hyperlipidemia on coronary vasodilator function and myocardial perfusion in regions having substantial impairment of baseline dilator reverse. Circulation 98:1291-1296, 1998

16. Brunel P, Bourassa MG, Wiseman A: Different rates of coronary disease progression in patients with normal and mildly disease coronary arteries. Coron Art Dis 2:449-454, 1991

17. Glover DK, Ruiz M, Edwards NC, et al: Comparison between Tl-201 and Tc-99m sestamibi uptake during adenosine induced vasodilation as a function of coronary artery severity. Circulation 91:813-820, 1995

18. Glover DK, Okada RD: Myocardial kinetics of Tc-MIBI in canine myocardium after dipyridamole. Circulation 81:628-637, 1990

19. Sinusas AJ, Shi QX, Saltzberg MT, et al: Technetium-99m tetrofosmin to assess myocardial blood flow: experimental validation in an intact canine model of ischemia. J Nucl Med 35:664-671, 1994

20. Hachamovich R, Berman DS, Kiat H, et al: Incremental prognostic value of adenosine stress myocardial perfusion single-photon emission computed tomography and impact on subsequent management in patients with or suspected of having myocardial ischemia. Am J Cardiol 80:426-433, 1997

21. DePuey EG, Rozanski A: Using gated technetium-99m-sestamibi SPECT to characterize fixed myocardial defects as infarct or artifact. J Nucl Med 36:952-955, 1995

22. Rigo P, VanBaxen P, Safi JF, et al: Quantitative evaluation of a comprehensive motion, resolution, and attenuation correction program: Initial experience. J Nucl Cardiol 5:458-468, 1998

23. O'Connor MK, Kemp B, Anstett F, et al: A multicenter evaluation of commercial attenuation compensation techniques in cardiac SPECT using phantom models. J Nucl Cardiol 9:361-376, 2002

24. Gould KL, Schelbert H, Phelps M, et al: Noninvasive assessment of coronary stenoses with myocardial perfusion imaging during pharmacologic coronary vasodilation. Am J Cardiol 43:200-208, 1979

25. Schelbert H, Wisenberg G, Phelps M, et al: Noninvasive assessment of coronary stenoses by myocardial imaging during pharmacological coronary vasodilation, VI: Detection of coronary artery disease in man with intravenous 14-NH$_3$ and positron computed tomography. Am J Cardiol 49:1197-1207, 1982

26. Tillisch J, Brunken R, Marshall R, et al: Reversibility of cardiac wall motion abnormalities predicted by positron emission tomography. N Engl J Med 314:884-888, 1986

27. Phelps ME, Cherry SR: The changing design of positron imaging systems. Clin Pos Imaging 1:31-45, 1988

28. Schelbert HR, Phelps ME, Hoffman EJ, et al: Regional myocardial perfusion assessed with N-13 labeled ammonia and positron emission computerized axial tomography. Am J Cardiol 43:209-218, 1979

29. Schelbert HR, Phelps ME, Huang SC, et al: N-13 ammonia as an indicator of myocardial blood flow. Circulation 63:1259-1272, 1981

30. Beanlands R, Muzik O, Hutchins G, et al: Heterogeneity of regional nitrogen 13-labeled ammonia tracer distribution in the normal heart: Comparison with rubidium-82 and copper-62-labeled PTSM. J Nucl Cardiol 35:1122-1124, 1994

31. Tamaki N, Ruddy TD, Dekamp R, et al: Myocardial perfusion, in Wahl RL, Buchanan JW, (eds): Principles and Practice of Positron Emission Tomography. Philadelphia, PA, Lippincott, Williams & Wilkins, 2002 pp 320-333

32. Bergmann SR, Fox KAA, Rand AL, et al: Quantification of regional myocardial blood flow in vivo with H$_2$15O. Circulation 70:724-733, 1984

33. Kim SH, Machac J, Almeida O, et al: Optimization of rubidium-82 generator performance. Clin Nucl Med 29:135P, 2004

34. Meerdink DJ, Leppo JA. Experimental studies of the physiologic properties of technetium-99m agents: Myocardial transport of perfusion imaging agents. Am J Cardiol 66:9E-15E, 1990

35. Leppo JA, Meerdink DJ: Comparison of the myocardial uptake of a

technetium-labeled isonitrile analogue and thallium. Circ Res 65:62-639, 1989

36. Mack RE, Nolting DD, Hogancamp CE, et al: Myocardial extraction of Rb-86 in the rabbit. Am J Physiol 197:1175-1177, 1959

37. Becker L, Ferreira R, Thomas M: Comparison of Rb-86 and microsphere estimates of left ventricular blood flow distribution. J Nucl Med 15:969-973,1977

38. Selwyn AP, Allan RM, L'Abbate A, et al: Relation between regional myocardial uptake of rubidium-82 and perfusion: Absolute reduction of cation uptake in ischemia. Am J Cardiol 50:112-121, 1982

39. Goldstein RA, Mullani NA, Marani SK, et al: Myocardial perfusion with rubidium-82. II. Effects of metabolic and pharmacological interventions. J Nucl Med 24:907-915, 1983

40. Schelbert HR, Ashburn WL, Chauncey DM, et al: Comparative myocardial uptake of intravenously administered radionuclides. J Nucl Med 15:1092-1100, 1977

41. Wyss CA, Koepfli P, Mikolajczyk K, et al: Bicycle exercise stress in PET for assessment in PET for assessment of coronary flow reserve: Repeatability and comparison with adenosine stress. J Nucl Med 33:146-154, 2003

42. Chow BJ, Ruddy TD, Dalipaj MM, et al: Feasibility of exercise rubidium-82 positron emission tomography myocardial perfusion imaging. J Am Coll Cardiol 41:428A, 2003

43. Machac J, Chen H, Almeida O, et al: Comparison of filtered back projection vs iterative reconstruction of rubidium-82 PET perfusion images. J Nucl Med 44:270P, 2003

44. Machac J, Chen H, Almeida OD, et al: comparison of 2D and high dose and low dose 3D gated myocardial Rb-82 PET imaging. J Nucl Med 43:P188, 2002

45. Knesaurek K, Machac J, Krynyckyi BR, et al: Comparison of 2-dimensional and 3-dimensional 82-Rb myocardial perfusion PET imaging. J Nucl Med 44:1350-1356, 2003

46. Cherry SR, Sorenson JA, Phelps ME (eds):Physics in Nuclear Medicine (ed 3). Philadelphia, Saunders, 2003, p 351

47. Moser KW, Case JA, Bateman TM, et al: A quantitative comparison of 2D and 3D acquisition of Rb-82 myocardial perfusion PET studies on an LSO scanner. J Nucl Med 45:222P, 2004

48. DiFilippo FP, Brunken RC, Neumann DR, et al: Initial clinical experience with Rb-82 cardiac PET imaging on a PET/CT system. J Nucl Med 45:117P, 2004

49. Machac J, Mosci K, Almeida OD, et al: Gated rubidium-82 cardiac PET imaging: Evaluation of left ventricular wall motion. J Amer Coll Cardiol 39:393A, 2002

50. Almeida O, Machac J, Travis A, et al: Measurement of left ventricular ejection fraction with gated cardiac rubidium-82 positron emission tomography. J Nucl Med 45:224P, 2004

51. Case JA, Bateman TM, Moser K, et al: comparison of LVEF measurements from ECG-gated Rb-82 myocardial perfusion PET and Tc-99m sestamibi myocardial perfusion SPECT. J Nucl Cardiol 10:S13, 2003

52. Hickey KT, Sciacca RR, Bokhari S, et al: Assessment of cardiac wall motion and ejection fraction with gated PET using N-13 ammonia. Clin Nucl Med 29:243-248, 2004

53. Cherry SR, Sorenson JA, Phelps ME (eds):Physics in Nuclear Medicine (ed 3). Philadelphia, Saunders, 2003, pp 299-324

54. Eisner RL, Patterson RE: Differences between women and men in the heterogeneity of myocardial perfusion images: SPECT Tl-201, Tc-99m sestamibi, and PET Rb-82. J Nucl Cardiol 4:S104, 1997

55. Patterson RE, Cloninger K, Churchwell KB, et al: Special problems with cardiovascular imaging in women, in Julian DG, Wenger NK (eds). Women and Heart Disease. London, Martin Dunitz Ltd. p 91, 1997

56. Curchwell KB, Pilcher WC, Eisner RL, et al: accuracy of Pet Rb MPI to diagnose coronary artery disease: New software for objective analysis. J Nucl Med 35:23P, 1994

57. Churchwell KB, Pilcher WC, Eisner RL, et al: Quantitative analysis of PET: The women's test for coronary disease. J Nucl Med 36:79P, 1995

58. Eisner RL, Tamas MJ, Cloninger K, et al: The normal SPECT thallium-201 bullseye display: Gender differences. J Nucl Med 29:1901-1909, 1989

59. Shonkoff D, Eisner RL, Gober A, et al: What quantitative criteria should be used to read defects on the SPECT Tl-201 bullseye display in men? ROC analysis. J Nucl Med 28:674-675P, 1987

60. DePuey EG, Rozanski A: Using gated technetium-99m-sestamibi SPECT to characterize fixed myocardial defects as infarct or artifact. J Nucl Med 36:952-955, 1995

61. Taillefer R, DePuye EG, Udelson JE, et al: comparative diagnostic accuracy of Tl-201 and Tc-99m sestamibi SPECT imaging (perfusion and ECG-gated SPECT) in detecting coronary artery disease in women. J Am Coll Cardiol 29:69-77, 1997

62. Choi JY, Lee KH, Kim SJ, et al: Gating provides improved accuracy for differentiating artifacts from true lesions in equivocal fixed defects on technetium 99m tetrofosmin perfusion SPECT. J Nucl Cardiol 5:395-401, 1998

63. Paola E, Smiano P, Watson DD, et al: Value of gating of technetium-99m sestamibi single photon emission tomographic imaging. J Am Coll Cardiol 30:1687-1692, 1997

64. Ficaro EP, Fessler JA, Shreve PD, et al: Simultaneous transmission/emission myocardial perfusion tomography: Diagnostic accuracy of attenuation—corrected 99mTc-sestamibi single photon emission computed tomography. Circulation 93:463-473, 1996

65. Hendel RC, Corbett JR, Cullom ST, et al: The value and practice of attenuation correction for myocardial perfusion SPECT imaging: A joint position paper from the American Society of Nuclear Cardiology and the Society of Nuclear Medicine. J Nucl Cardiol 9:135-143, 2002

66. O'Connor MK, Kemp B, Anstett F, et al: A multicenter evaluation of commercial attenuation compensation techniques in cardiac SPECT using phantom models. J Nucl Cardiol 9:361-376, 2002

67. DePuey EG, Rozanski A: Using gated technetium-99m-sestamibi SPECT to characterize fixed myocardial defects as infarct or artifact. J Nucl Med 36:952-955, 1995

68. Taillefer R, DePuey EG, Udelson JE, et al: Comparative diagnostic accuracy of thallium-201 and Tc-99m sestamibi SPECT imaging (perfusion and ECG-gated SPECT) in detecting coronary artery disease in women. J Am Coll Cardiol 29:69-77, 1997

69. Hansen CL, Crabbe D, Rubin S: Lower diagnostic accuracy of thallium-201 SPECT myocardial perfusion in women: An effect of smaller chamber size. J Am Coll Cardiol 28:1214-1219, 1996

70. Williams B: Women and coronary disease: Is PET rubidium-82 imaging the preferred noninvasive diagnostic test? Appl Imaging Appl Nucl Cardiol 1:1-4, 2000

71. Patterson RE, Churchwell KB, Eisner RL: Diagnosis of coronary artery disease in women: Roles of three-dimensional imaging with magnetic resonance imaging or positron emission tomography. Am J Cardiac Imaging 10:78-88, 1996

72. Flegal KM, Carroll MD, Ogden CL, et al: Prevalence and trends in obesity among US adults, 1999-2000 JAMA 288:1723-1727, 2002.

73. Patterson RE, Cloninger K, Churchwell KB, et al: Special problems with cardiovascular imaging in women, in Julian DG, Wenger NK (eds). Women and Heart Disease. London: Martin Dunitz Ltd. pp 91, 1997

74. Bateman TM: PET myocardial perfusion imaging: Making the transition to a clinical routine. Appl Imaging 3:1-6, 2002

75. Imaging Technology News, 6:2004, Reilly communications group

76. Yoshinaga K, Chow B, DeKemp Robert, et al: prognostic value of rubidium-82 perfusion positron emission tomography: Preliminary results from the consecutive 153 patients. J Am Coll Cardiol 43:338A, 2004

77. VanTosh A, Supino PG, Simulever RP, et al: Normal PET myocardial perfusion imaging in women with chest pain predicts a low cardiovascular event rate and favorable long term clinical outcome. J Am Coll Cardiol 37:381A, 2001

78. Valensi P, Sachs R, Cosson E, et al: prognostic value of epicardial coronary artery constriction to cold pressor test in type 2 diabetic patients with angiographically normal coronary arteries and no other major coronary risk factors. Diabetes Care 27:208, 2004

79. Dorbala S, Mishra R, Logsetty G, et al: PET measurements of coronary flow reserve identify individuals at high risk of developing clinically apparent coronary artery disease (CAD). J Nucl Med 45:236P, 2004

80. Merhige ME, Watson GM, Oliverio JG, et al: Efficacy of lipid lowering therapy in inducing arrest or reversal of coronary disease as assessed with positron emission tomography. J Am Coll Cardiol 43:332A, 2004

81. Kern MJ, Anderson HV: A symposium: The clinical applications of the intracoronary Doppler guidewire flow velocity in patients: Understanding blood flow beyond the coronary stenosis. Am J Cardiol 71: 1D-70D, 1993

82. Gould KL, Nakagawa Y, Nakagawa K, et al: Frequency and clinical implications of fluid dynamically significant diffuse coronary artery disease manifest as graded, longitudinal, base-to-apex myocardial perfusion abnormalities by noninvasive positron emission tomography. Circulation 101:1931-1939, 2000

83. Hernandez-Pampaloni M, Keng FY, Kudo T, et al: Abnormal longitudinal, base-to-apex myocardial perfusion gradient by quantitative blood flow measurements in patients with coronary risk factors. Circulation 104:527-532, 2001

84. Bergmann SR, Fox KAA, Rand AL, et al: Quantification of regional myocardial blood flow in vivo with $H_2^{15}O$. Circulation 70:724-733, 1984

85. DiCarli M, Czernin J, Hoh CK, et al: Relation among stenosis severity, myocardial blood flow, and flow reserve in patients with coronary artery disease. Circulation 91:1944-1951, 1995

86. Nagamachi S, Czernin J, Kim AS, et al: Reproducibility of measurements of regional resting and hyperemic myocardial blood flow assessed with PET. J Nucl Med 37:1626-1631, 1996

87. Sawada S, Muzik O, Beanlands RS, et al: Interobserver and interstudy variability of myocardial blood flow and flow-reserve measurements with nitrogen 13 ammonia-labeled positron emission tomography. J Nucl Cardiol. 2:413-422, 1995

88. Machac J, Knesaurek K, Chen H, et al: Validation of a practical method of coronary flow reserve quantification with rubidium-82 myocardial PET perfusion imaging. J Nucl Med 44:P90, 2003

89. Lin JW, Sciacca RR, Chou RL, et al: Quantification of myocardial perfusion in human subjects using Rb-82 and wavelet-based noise reduction. J Nucl Med 42:201-208, 2001

90. Demer LL, Gould KL, Westcot RJ, et al: Noninvasive assessment of coronary artery collaterals in man by PET perfusion imaging. J Nucl Med 31:259-270, 1990

91. Garza D, Tosh AV, Roberti R, et al: Detection of coronary collaterals using dipyridamole PET myocardial perfusion imaging with rubidium-82. J Nucl Med 38:38-43, 1997

92. Goldstein RA, Haynie M: Limited myocardial perfusion reserve in patients with left ventricular hypertrophy. J Nucl Med 31:255-258, 1990

93. Yoshida K, Mullani N,k Gould KL: Coronary flow and flow reserve by PET simplified for clinical applications using rubidium-82 or nitrogen-13 ammonia. J Nucl Med 37:1701-1712, 1996

94. Mullani NA, Goldstein RA, Gould KL, et al: Myocardial perfusion with rubidium-82. I. Measurement of extraction fraction and flow with external detectors. J Nucl Med 24:898-906, 1983

95. Goldstein RA, Mullani NA, Fisher D, et al: Myocardial perfusion with rubidium-82. II. The effects of metabolic and pharmacologic interventions. J Nucl Med 24:907-915, 1983

96. Machac J, Knesaurek K, Chen H, et al: Validation of a practical method of coronary flow reserve quantification with rubidium-82 myocardial PET perfusion imaging. J Nucl Med 44:P90, 2003

97. DeKemp RA, Ruddy TD, Hewitt T, et al: Detection of serial changes in absolute myocardial perfusion with 82Rb PET. J Nucl Med 41:1426-1435, 2000

98. Yokoyama I, Momomura S, Ohtake T, et al: Improvement of impaired myocardial vasodilation due to diffuse coronary sclerosis in hypercholesterolemics after lipid-lowering therapy. Circulation 100:117-122, 1999

99. Huggins GS, Pasternak RC, Alpert NM, et al: Effects of short-term treatment of hyperlipidemia on coronary vasodilator function and myocardial perfusion in regions having substantial impairment of baseline dilator reverse. Circulation 98:1291-1296, 1998

100. Henzlova MJ, Machac J, Squire A, et al: Screening for the presence of coronary artery disease in patients with end stage liver disease using SPECT and PET imaging: Is dipyridamole a good stressor? J Nucl Cardiol 10:S5, 2003

101. Machac J, Travis A, Almeida O, et al: Is coronary flow reserve decreased in patients with end-stage liver disease? J Nucl Med 45:P238, 2004

102. Mishra RK, Sciammarella M, Dorbala S, et al: Do changes in hemodynamics during intravenous adenosine infusion predict the magnitude of coronary hyperemia? J Nucl Med 45:4P, 2004

103. Parkash R, DeKamp RA, Ruddy TD, et al: Potential utility of rubidium 82 PET quantification in patients with 3-vessel coronary artery disease. J Nucl Cardiol 11:440-449, 2004

104. Muzik O, Beanlands RSB, Hutchins GD, et al: Validation of nitrogen-13-ammonia tracer kinetic model for quantification of myocardial blood flow using PET. J Nucl Med 34:83-91, 1993

105. DiCarli M, Czernin J, Hoh CK, et al: Relation among stenosis severity, myocardial blood flow, and flow reserve in patients with coronary artery disease. Circulation 91:1944-1951, 1995

106. Gould KL, Lipscomb K, Hamilton GW: Physiological basis for assessing critical coronary stenosis. Am J Cardiol 33:87-94, 1974

107. Khouri EM, Gregg DE, Lowensohn HS: Flow in the major branches of the left coronary artery during experimental coronary insufficiency in the unanesthetized dog. Circ Res 23:99-109, 1968

108. Uren NG, Melin JA, DeBruyne B, et al: Relation between myocardial blood flow and the severity of coronary artery-stenosis. N Engl J Med 330:1782-1788, 1994

109. Bache RJ, Cobb FR: Effect of maximal coronary vasodilation on transmural myocardial perfusion during tachycardia in the awake dog. Circ Res 41:648-653, 1977

110. McGinn AL, White CW, Wilson RF: Intersudy variability of coronary flow reserve: Influence of heart rate, arterial blood pressure, and ventricular preload. Circulation 81:1319-1330, 1990

111. Rossen JD, Winniford MD: Effect of increases in heart rate and arterial pressure on coronary flow reserve in humans. J Am Coll Cardiol 21:343-348, 1993

112. Hoffman JIE: Maximal coronary flow and the concept of coronary vascular reserve. Circulation 70:153-173, 1984

113. Demer LL, Gould KL, Westcot RJ, et al: Noninvasive assessment of coronary artery collaterals in man by PET perfusion imaging. J Nucl Med 31:259-270, 1990

114. Garza D, Tosh AV, Roberti R, et al: Detection of coronary collaterals using dipyridamole PET myocardial perfusion imaging with rubidium-82. J Nucl Med 38:38-43, 1997

115. Akinboboye OO, Idris O, Chou RL, et al: Absolute quantification of coronary artery steal induced by intravenous dipyridamole. J Am Coll Cardiol 37:109-116, 2001

116. Yokoyama I, Momomura S, Ohtake T, et al: Improvement of impaired myocardial vasodilation due to diffuse coronary sclerosis in hypercholesterolemics after lipid-lowering therapy. Circulation 100:117-122, 1999

117. Pethig K, Heublein B, Meliss RR, et al : Volumetric remodeling of the proximal left coronary artery: Early versus late after heart transplantation. J Am Coll Cardiol 34:197-203, 1999

118. Zanco P, Gambino A, Livi U, et al: Changes in myocardial blood flow (MBF) and coronary reserve (CR) evaluated by PET early and late heart transplant. J Nucl Med 41:41P, 2000

119. Sdringola S, Nakagawa K, Nakagawa Y, et al: Combined lifestyle and pharmacologic lipid treatment further reduce coronary events and myocardial perfusion abnormalities compared with usual-care cholesterol-lowering drugs in coronary artery disease. J Am Coll Cardiol 41:263-272, 2003

120. Gould KL, Ornish D, Scherwitz L, et al: Changes in myocardial perfusion abnormalities by positron emission tomography after long-term, intense risk factor modification. JAMA 275:1402-1403, 1996

121. Yokoyama I, Momomura S, Ohtake T, et al: Improvement of impaired myocardial vasodilation due to diffuse coronary sclerosis in hypercholesterolemics after lipid-lowering therapy. Circulation 100:117-122, 1999

122. Uren NG, Marraccini P, Gistri R, et al: Altered coronary vasodilator

reserve and metabolism in myocardium subtended by normal arteries in patients with coronary artery disease. J Am Coll Cardiol 22:650-658, 1993

123. Zeiher AM, Drexler H, Wollschlager H, et al: Endothelial dysfunction of the coronary microvasculature is associated with impaired coronary flow regulation in patients with early atherosclerosis. Circulation 84: 1984-1992, 1991

124. Yoshinaga K, Katoh C, Noriyasu K, et al: Reduction of coronary flow reserve in areas with and without ischemia on stress perfusion imaging in patients with coronary artery disease: A study using oxygen 15-labeled water PET. J Nucl Cardiol 10:275-83, 2003

125. Brunel P, Bourassa MG, Wiseman A: Different rates of coronary disease progression in patients with normal and mildly disease coronary arteries. Coronary Artery Dis 2:449-454, 1991

126. Sdringola S, Patel D, Gould KL: High prevalence of myocardial perfusion abnormalities on positron emission tomography in asymptomatic persons with a parent of sibling with coronary artery disease. Circulation 103:496-501, 2001

127. Rajappan K, Rimoldi O, Shafers KP, et al: Evidence of stress-induced subendocardial hypoperfusion in patients with aortic stenosis demonstrated by positron emission tomography. J Am Coll Cardiol 37: 419A, 2001

128. Yokoyama I, Momomura S, Ohtake T, et al: Improvement of impaired myocardial vasodilation due to diffuse coronary sclerosis in hypercholesterolemics after lipid-lowering therapy. Circulation 100:117-122, 1999

129. Huggins GS, Pasternak RC, Alpert NM, et al: Effects of short-term treatment of hyperlipidemia on coronary vasodilator function and myocardial perfusion in regions having substantial impairment of baseline dilator reverse. Circulation 98:1291-1296, 1998

130. Yokoyama I: Improvement of myocardial flow reserve after successful improvement of hyperglycemia in non-insulin dependent diabetics (NIDDM) was more prominent in NIDDM with coronary artery disease rather than in NIDDM with chest pain syndrome. J Nucl Med 40:168P, 1999

131. Czernin J, Barnard RJ, Sun KT, et al: Effect of short-term cardiovascular conditioning and low-fat diet on myocardial blood flow and flow reserve. Circulation 92:197-204, 1995

132. Helle T, Laaksonen R, Vesalainen R, et al: The effect of pravastatin on myocardial blood flow in young healthy adults. J Am Coll Cardiol 35:418A, 2000

133. Drexler H: Endothelial dysfunction: clinical implications. Prog Cardiovasc Dis 39:287-324, 1997

134. Schachinger V, Britten MB, Zeiher AM: Prognostic impact of coronary vasodilator dysfunction on adverse long-term outcome of coronary hear disease. Circulation 101:1899-1906, 2000

135. Halcox JP, Schenke WH, Zalos G, et al: prognostic value of coronary vascular endothelial dysfunction. Circulation 106:653-658, 2002

136. Schindler T, Hornig B, Buser PET, et al: prognostic value of abnormal reactivity of epicardial coronary arteries to sympathetic stimulation in patients with normal coronary angiograms. Arterioscler Thromb Vasc Biol 23:495-501, 2003

137. Andersen TJ, Meredith IT, Yeung AC, et al: The effect of cholesterol lowering and antioxidant therapy on endothelium-dependent coronary vasomotion. N Engl J Med 332:488-493, 1995

138. Zeiher AM, Drexler H, Wollschlager H, et al: Modulation of coronary vasomotor tone in humans: Progressive endothelial dysfunction with different early stages of coronary atherosclerosis. Circulation 83:391-401, 1991

139. Sendowski I, Savourey G, Launsay JC, et al: Sympathetic stimulation induced by hand cooling alters cold-induced vasodilation in humans. Eur J Appl Physiol 81:303-309, 2000

140. Heusch G, Baumgart D, Camici P, et al: Alpha-adrenergic coronary vasoconstriction and myocardial ischemia in humans. Circulation 101:689-694, 2001

141. Baumgart D, Naber C, Haude M, et al: G protein beta3 subunit 825T allele and enhanced coronary vasoconstriction on alpha(2)-adrenoreceptor activation. Circ Res 85:965-969, 1999

142. Zeiher AM, Drexler H, Wollschlager H, et al: Coronary vasomotion in

response to sympathetic stimulation in humans: Importance of the functional integrity of the endothelium. J Am Coll Cardiol 14:1181-1190, 1989

143. Schindler TH, Nitzsche EU, Olschewski M, et al: PET-measured responses of MBF to cold pressor testing correlated with indices of coronary vasomotion on quantitative coronary angiography. J Nucl Med 45:419-428, 2004

144. Schindler TH, Nitzche EU, Dacta AD, et al: Abnormal longitudinal base-to-apex myocardial perfusion gradient in response to cold-pressure test as assessed by PET correlates with indices of epicardial vasomotion on quantitative angiography. J Nucl Med 45:2P, 2004

145. Lanza GA, Manzoli A, Pasceri V, et al: Ischemic-like ST-segment changes during Holter monitoring in patients with angina pectoris and normal coronary arteries but negative exercise testing. Am J Cardiol 79:1-6, 1997

146. Schindler TH, Nitzsche E, Magosaki N, et al: Regional myocardial perfusion defects during exercise, as assessed by three-dimensional integration of morphology and function, in relation to abnormal endothelium-dependent vasoreactivity of the coronary microcirculation. Heart 89:517-526, 2003

147. Zeiher AM, Krause T, Schachinger V, et al: Impaired endothelium-dependent vasodilation of coronary resistance vessels is associated with exercise-induced myocardial ischemia. Circulation 91:2345-2352, 1995

148. Nabel EG, Ganz P, Gordon JB, et al: dilation of normal and constriction of atherosclerotic coronary arteries cause by the cold-pressor test. Circulation 77:43-52, 1988

149. Zeiher AM, Drexler H, Saurbier B, et al: Endothelium-mediated coronary blood flow modulation in humans: Effects of age, atherosclerosis, hypercholesterolemia, and hypertension. J Clin Invest 92:652-662, 1993

150. Schindler TH, Nitzsche EU, Olschewski M, et al: PET-measured responses of MBF to cold pressor testing correlated with indices of coronary vasomotion on quantitative coronary angiography. J Nucl Med 45:419-428, 2004

151. Quinones MJ, Hernandez-Pampaloni M, Schelbert H, et al: Coronary vasomotor abnormalities in insulin-resistant individuals. Ann Intern Med 140:700-708, 2004

152. Nitenberg A, Ledoux S, Valensi P, Sachs R, et al: Impairment of coronary microvascular dilation in response to cold-pressor induced sympathetic stimulation in type 2 diabetic patients with abnormal stress-thallium imaging. Diabetes 50:1180-1185, 2001

153. Momose M, Abletshauser C, Neverve J, et al: Dysregulation of coronary microvascular reactivity in asymptomatic patients with type 2 diabetes mellitus. Eur J Nucl Med 29:1675-1679, 2002

154. Schindler TH, Nitzche EU, Olschewski M, et al: Chronic inflammation and impaired coronary vasoreactivity in patients with coronary risk factors. J Nucl Med 45:7P, 2004

155. Schindler TH, Facta AD, Quinones MJ, et al: Metabolic syndrome is associated with abnormal coronary circulatory functions as measured by N-13 ammonia and PET. J Nucl Med 45:65P, 2004

156. Schindler TH, Facta AD, Prior JO, et al: Association of serum leptin levels and coronary vasomotor function in obesity. J Nucl Med 45: 64P, 2004

157. Campisi R, Czernin J, Schoder H, et al: L-arginine normalizes coronary vasomotion in long-term smokers. Circulation 99:491-497, 1999

158. Schindler TH, Magosaki N, Jeserich M, et al: Effect of ascorbic acid on endothelial dysfunction of epicardial coronary arteries in chronic smokers assessed by cold-pressor testing. Cardiology 94:239-246, 2000

159. Schindler TH, Nitzsche EU, Munzel T, et al: Coronary vasoregulation in patients with various risk factors in response to cold-pressor testing: Contrasting myocardial blood flow responses to short- and long-term vitamin C administration. J Am Coll Cardiol 42:814-822, 2003

160. Morita K, Noriyasu K, Tsukamoto T, et al: Reversible endothelial dysfunction after one month smoking cessation in healthy young smokers. J Nucl Med 45:3P, 2004

161. Facta AD, Schindler TH, Prior JO, et al: Noninvasively measured

myocardial blood flow responses to sympathetic stimulation may allow assessment of glucose control in type 2 diabetes. J Nucl Med 45:236P, 2004

162. DiCarli MF, Alfonso L, Campisi R, et al: Coronary vascular dysfunction in premenopausal women with diabetes mellitus. Am Heart J 144:711-718, 2002

163. Campisi R, Nathan L, Pampaloni MH, et al: Noninvasive assessment of coronary microcirculatory function in post-menopausal women and effects of short-term and long-term estrogen administration. Circulation 105:E9069-E9070, 2002

164. Jensen LO, Thayssen P, Pedersen KE, et al: Regression of coronary atherosclerosis by simvastatin: A serial intravascular ultrasound study. Circulation 110:265-270, 2004

165. Prior JO, Facta AD, Schindler TH, et al: Effect of the number of criteria of the metabolic syndrome on coronary circulatory function as measured by N-13 ammonia and PET. J Nucl Med 45:237P, 2004

166. Kjaer A, Meyer C, Nielsen FS, et al: Dipyridamole, cold pressor test, and demonstration of endothelial dysfunction: A PET study of myocardial perfusion in diabetes. J Nucl Med 44:19-23, 2003

167. Bonetti PO, Lerman LO, Lerman A: Endothelial dysfunction: A marker of atherosclerotic risk. Arterioscler Thromb Vasc Biol 23:168-175, 2003

168. Loscalzo J: Functional polymorphisms in a candidate gene for atherothrombosis: Unraveling the complex fabric of a polygenic phenotype. J Am Coll Cardiol 41:946-948, 2003

169. Schachinger V, Britten MB, Zeiher AM: Prognostic impact of coronary vasodilator dysfunction on adverse long-term outcome of coronary hear disease. Circulation 101:1899-1906, 2000

170. Gould KL, Goldstein RA, Mullani NA: Economic analysis of clinical positron emission tomography of the heart with rubidium-82. J Nucl Med 30:707-717, 1989

171. Gould KL: Goal, gold standards and accuracy of non-invasive myocardial perfusion imaging for identifying and assessing severity of coronary artery disease. Curr Opin Cardiol 4:834-844, 1989

172. Gould KL, Mullani NA, Williams B: PET, PTCA, and economic priorities. Clin Cardiol 13:153-164, 1990

173. Patterson RE, Eisner RL, Horowitz SF, et al: comparison of cost-effectiveness and utility of exercise ECG, single photon emission tomography, and coronary angiography for diagnosis of coronary artery disease. Circulation 91:54-65, 1995

174. Merhige ME: PET myocardial perfusion imaging: A new standard for the management of coronary artery disease. Appl Imaging 191:1-4, 2000

175. Patterson RE, Eisner RL, Horowitz SF, et al: comparison of cost-effectiveness and utility of exercise ECG, single photon emission tomography, and coronary angiography for diagnosis of coronary artery disease. Circulation 91:54-65, 1995

176. DiCarli MF, Asgazadie F, Schelbert HR, et al: Relation of myocardial perfusion at rest and during pharmacologic stress to the PET patterns of tissue viability in patients with severe left ventricular dysfunction. J Nucl Cardiol 5:558-566, 1998

177. DiCarli M, Asgarzadie F, Schelbert HR, et al: Quantitative relation between myocardial viability and improvement in heart failure symptoms after revascularization in patients with ischemic cardiomyopathy. Circulation 92:3436-3444, 1995

178. DiCarli MF, Davidson M, Little R, et al: Value of metabolic imaging with positron emission tomography for evaluating prognosis in patients with coronary artery disease and left ventricular dysfunction. Am J Cardiol 73:527-533, 1994

179. Eitzman D, al-Aouar Z, Kanter HL, et al: Clinical outcome of patients with advanced coronary artery disease after viability studies with positron emission tomography. J Am Coll Cardiol 20:559-565, 1992

180. Kron IL, Flanagan TL, Blackbourne LH, et al: Coronary revascularization rather than cardiac transplantation for chronic ischemic cardiomyopathy. Ann Surg 210:348-352, 1989

181. Lee KS, Marwick TH, Cook SA, et al: Prognosis of patients with left ventricular dysfunction, with or without viable myocardium after myocardial infarction. Relative efficacy of medical therapy and revascularization. 90:2687-2694, 1994

182. Yoshida D, Gould KL: Quantitative relation of myocardial infarct size and myocardial viability by positron emission tomography to left ventricular ejection fraction and 3-year mortality with and without revascularization. J Am Coll Cardiol 22:984-997, 1993

183. vom Dahl J, Altehoefer C, Sheehan FH, et al: Effect of myocardial viability assessed by technetium-99m-sestamibi SPECT and fluorine-18-FDG PET on clinical outcome in coronary artery disease. J Nucl Med 38:742-748, 1997

184. Tillisch J, Brunken R, Marshall R, et al: Reversibility of cardiac wall motion abnormalities predicted by positron emission tomography. N Engl J Med 314:884-888, 1986

185. Srinivasan G, Kitsiou AN, Bacharach SL, et al: F-18 fluorodeoxyglucose single photon enission computed tomography: Can it replace PET and thallium SPECT for the assessment of myocardial viability? Circulation 97:843-850, 1998

186. Arrhighi JA, CK NG, Dey HM, et al: Effect of left ventricular function on the assessment of myocardial viability by technetium-99m sestamibi and correlation with positron tomography in patients with healed myocardial infarcts of stable angina pectoris, or both. Am J Cardiol 80:1007-1013, 1997

187. Hernandez-Pampaloni M, Allada V, Fishbein MC, et al: Myocardial perfusion and viability by positron emission tomography in infants and children with coronary abnormalities: Correlation with echocardiography, coronary angiography, and histopathology. J Am Coll Cardiol 41:618-626, 2003

188. Bacharach SL, Bax JJ, Case J, et al: PET myocardial glucose metabolism and perfusion imaging. Part I-Guidelines for patient preparation and data acquisition. J Nucl Cardiol 10:543-554, 2003

189. Dilsizian V, Arrighi JA, Diodati JG, et al: Myocardial viability in patients with chronic coronary artery disease. Comparison of 99m Tc-sestamibi with thallium reinjection and 18-F fluorodeoxyglucose. Circulation 89:578-587, 1994

190. Goldstein RA: Kinetics of rubidium-82 after coronary occlusion and reperfusion. J Clin Invest 75:1131-1137, 1985

191. Gould KL, Haynie M, Hess MJ, et al: Myocardial metabolism of fluorodeoxyglucose compared to cell membrane integrity for the potassium analog Rb-82 for assessing viability and infarct size in man by PET. J Nucl Med 31:1-9, 1990

192. Gould KL, Yoshida K, Hess MJ, et al: Myocardial metabolism of fluorodeoxyglucose compared to cell membrane integrity for the potassium analogue rubidium-82 for assessing infarct size in man by PET. J Nucl Med 32:1-9, 1991

193. VomDahl J, Muzik O, Wolfe ER, et al: Myocardial ubidium-82 tissue kinetics assessed by dynamic positron emission tomography as a marker of myocardial cell membrane integrity and viability. Circulation 93:238-245, 1996

194. Almeida O, Machac J, Knesaurek K, et al: The predictive value of rest and stress rubidium-82 washout for the determination of myocardial viability. J Nucl Med 44:P7, 2003

195. Beanlands RS, DeKemp R, Scheffel A, et al: Can nitrogen-13 ammonia kinetic modeling define myocardial viability independent of fluorine-18 fluorodeoxyglucose? J Am Coll Cardiol 29:537-543, 1997

196. Chan P, Machac J, Almeida O, et al: The prevalence and impact of vertical heart movement during rest and stress rubidium-82 cardiac PET imaging. J Nucl Med 44:210-211P, 2003

197. Loghin C, Sdringola S, Gould KL: Common artifacts in PET myocardial perfusion images due to attenuation-emission misregistration: Clinical significance, causes, and solution. J Nucl Med 45:1029-1039, 2004

198. Chan P, Machac J, Almeida O, et al: The prevalence and impact of vertical heart movement during rest and stress rubidium-82 cardiac PET imaging. J Nucl Med 44:210-211P, 2003

199. DiFilippo FP, Brunken RC, Neumann DR, et al: Initial clinical experience with Rb-82 cardiac PET imaging on a PET/CT system. J Nucl Med 45:117P, 2004

200. DiCarli MF, Dorbala S, Mishra R, et al: Clinical myocardial perfusion PET/CT imaging with rubidium-82: Initial experience in 94 patients. J Nucl Med 45:117P, 2004

201. DiCarli MF, Dorbala S, Mishra R, et al: Clinical myocardial perfusion

PET/CT imaging with rubidium-82: Initial experience in 94 patients. J Nucl Med 45:117P, 2004

202. Wassenaar RW, Wells RG, DeKemp R, et al: Clinical evaluation of CT versus Ge-68 attenuation correction in cardiac PET imaging. J Nucl Med 45:118P, 2004

203. Stanger R, Jana S, Mistein D, et al: Accuracy of CT transmission maps in PET imaging studies. J Nucl Med 45:41P, 2004

204. Brunken RC, DiFilippo FP, Bybel B, et al: Clinical evaluation of cardiac PET attenuation correction using "fast" and "slow" CT images. J Nucl Med 45:120P, 2004

205. Erdi YE, Pevsner K, Rosenzweig E, et al: 4D-PET/CT acquisition in the thorax. J Nucl Med 45:48P, 2004

206. Kim JH, Czernin J, Auerbach M, et al: Mutual information software fusion of PET and CT improves image coregistration of in-line PET/CT images. J Nucl Med 48P, 2004

207. Quantitation of respiratory motion during 4D PET/CT acquisition. J Nucl Med 45:49P, 2004

208. Facta AD, Prior JO, Schindler TH, et al: Coronary vasomotor function by PET and coronary calcification by EBT in normals and diabetics. J Nucl Med 45:240-241P, 2004

209. Prior JO, Facta AD, Schindler TH, et al: Severe coronary artery calcification by electron beam computed tomography (EBCT) in asymptomatic subjects is not correlated with coronary circulatory dysfunction as measured by PET. J Nucl Med 45:108P, 2004

210. Glass ED, Ashby SP, Khoury JD, et al: Comparison of myocardial perfusion imaging with coronary calcium and angiography by multidetector CT. J Nucl Med 45:108P, 2004

211. Ropers D, Baum U, Phle K, et al: Detection of coronary artery stenoses with thin-slice multidetector row spiral computed tomography and multiplanar reconstruction. Circulation 107:664-666, 2003

212. Paul JF, Ohanessian A, Caussin Ch, et al: Visualization of coronary tree and detection of coronary artery stenosis using 16-slice, sub-millimeter computed tomography: Preliminary experience. Arch Mal Coeur Vaiss 97:31-36, 2004

213. Namdar M, Hany TF, Siegrist PT, et al: Improved CAD assessment using a combined PET.CT scanner. J Nucl Med 45:117P, 2004

214. Faber TL, Garcia EV, Hertel S, et al: Evaluation of automatic fusion of coronary arteries onto left ventricular surfaces from PET/CT. J Nucl Med 45:399P, 2004

215. Cherry SR, Sorenson JA, and Phelps ME Physics in Nuclear Medicine (ed 3). Philadelphia, Saunders, 2003, p 331

216. Cho ZH, Chan JK, Ericksson L, et al: Positron ranges obtained from biomedically important positron-emitting radionuclides. J Nucl Med 16:1174-1176, 1975

217. Phelps ME, Hoffman EJ, Huang SC, et al: Effect of positron range on spatial resolution. J Nucl Med 16:649-652, 1975

218. Derenzo SE, Budinger TF: Resolution limit for positron imaging devices. J Nucl Med 18:491-492, 1977

219. Schelbert HR, Phelps ME, Huang SC, et al: N-13 ammonia as an indicator of myocardial blood flow. Circulation 63:1259-1272, 1981

220. Mullani NA, Goldstein RA, Gould KL: Myocardial perfusion with rubidium-82. I- Measurement of extraction fraction and flow with external detectors. J Nucl Med 24:898-906, 1983

221. Schelbert HR, Schwaiger M: PET studies of the heart, in Phelps ME, Mazziotta JC, Schelbert HR (eds): Positron Emission Tomography and Autoradiography, Principles and Applications for the Brain and Heart. New York, Raven Press, 1986, pp 581-661

222. Stabin MG, Stubbs JB, Toohey RE: Radiation dose estimates for radiopharmaceutical. Radiation Dose Information Center, Oak Ridge, TN, Oak Ridge Institute for Science and Education, 1996, pp 10-28

223. Bateman TM: PET myocardial perfusion imaging: Making the transition to a clinical routine. Appl Imaging 3:1-6, 2002

224. Gould KL, Goldstein RA, Mullani NA, et al: Noninvasive assessment of coronary stenoses by myocardial perfusion imaging during pharmacologic coronary vasodilation. VIII. Clinical feasibility of positron cardiac imaging without a cyclotron using generator produced rubidium-82. Am J Cardiol 7:775-789, 1986

225. Demer LL, Gould KL, Goldstein RA, et al: Assessment of coronary artery disease severity by positron emission tomography: Comparison with quantitative arteriography in 193 patients. Circulation 79:825-835, 1989

226. Go R, Marwick T, MacIntyre W, et al: A prospective comparison of rubidium-82 PET and thallium-201 SPECT myocardial perfusion imaging utilizing a single dipyridamole stress in the diagnosis of coronary artery disease. J Nucl Med 31:1899-1905, 1990

227. Schelbert H, Wisenberg G, Phelps M, et al: Noninvasive assessment of coronary stenoses by myocardial imaging during pharmacological coronary vasodilation, VI: Detection of coronary artery disease in man with intravenous 14-NH₃ and positron computed tomography. Am J Cardiol 49:1197-1207, 1982

228. Yonekura Y, Tamaki N, Senda M, et al: Detection of coronary artery disease with 13-N ammonia and high resolution positron-emission computed tomography. Am Heart J 113:645-654, 1987

229. Williams B, Jansen D, Wong L, et al: Positron emission tomography for the diagnosis of coronary artery disease: A non-university experience and correlation with coronary angiography. J Nucl Med 30:845, 1989

230. Stewart RE, Schwaiger M, Molina E, et al: Comparison of rubidium-82 positron emission tomography and thallium-201 SPECT imaging for detection of coronary artery disease. Am J Cardiol 67:1303-1310, 1991

231. Tamaki N, Yonekura Y, Senda M, et al: Value and limitations of stress thallium-201 single photon emission computed tomography: Comparison with nitrogen-13 ammonia positron tomography. J Nucl Med 29:1181-1188, 1988

232. Go R, Marwick T, MacIntyre W, et al: A prospective comparison of rubidium-82 PET and thallium-201 SPECT myocardial perfusion imaging utilizing a single dipyridamole stress in the diagnosis of coronary artery disease. J Nucl Med 31:1899-1905, 1990

233. Stewart RE, Schwaiger M, Molina E, et al: Comparison of rubidium-82 positron emission tomography and thallium-201 SPECT imaging for detection of coronary artery disease. Am J Cardiol 67:1303-1310, 1991

234. Tamaki N, Yonekura Y, Senda M, et al: Value and limitations of stress thallium-201 single photon emission computed tomography: Comparison with nitrogen-13 ammonia positron tomography. J Nucl Med 29:1181-1188, 1988

235. Flegal KM, Carroll MD, Ogden CL, et al: Prevalence and trends in obesity among US adults, 1999-2000 JAMA 288:1723-1727, 2002.

236. Almeida O, Machac J, Travis A, et al: Measurement of left ventricular ejection fraction with gated cardiac rubidium-82 positron emission tomography. J Nucl Med 45:224P, 2004

237. Gould KL, Nakagawa Y, Nakagawa K, et al: Frequency and clinical implications of fluid dynamically significant diffuse coronary artery disease manifest as graded, longitudinal, base-to-apex myocardial perfusion abnormalities by noninvasive positron emission tomography. Circulation 101:1931-1939, 2000

238. Gould KL, Goldstein RA, Mullani NA: Economic analysis of clinical positron emission tomography of the heart with rubidium-82. J Nucl Med 30:707-717, 1989

239. Gould KL, Haynie M, Hess MJ, et al: Myocardial metabolism of fluorodeoxyglucose compared to cell membrane integrity for the potassium analog Rb-82 for assessing viability and infarct size in man by PET. J Nucl Med 31:1-9, 1990

240. Package Insert for Cardiogen-82, Internal Dosimetry Center at Oak Ridge Associated Universities, Bracco Diagnostics, Princeton, NJ

241. Bateman TM, McGhie AI, Heller GV, et al: ECG-Gated rubidium-82 perfusion PET imaging: A multiexpert comparison with technetium-99m sestamibi SPECT. Circulation 110:III-611, 2004